

## **Distribution Agreement**

In presenting this thesis as a partial fulfillment of the requirements for a degree from Emory University, I hereby grant to Emory University and its agents the non-exclusive license to archive, make accessible, and display my thesis in whole or in part in all forms of media, now or hereafter now, including display on the World Wide Web. I understand that I may select some access restrictions as part of the online submission of this thesis. I retain all ownership rights to the copyright of the thesis. I also retain the right to use in future works (such as articles or books) all or part of this thesis.

Hugh W. Phillis

April 6, 2017

Investigating *in utero* Fertilization, *in vitro* Fertilization, and the Mermaid-2 Voltage Sensor in  
*Caenorhabditis elegans*

by

Hugh W. Phillis

Dr. Steven W. L'Hernault  
Adviser

Department of Physics

Dr. Steven W. L'Hernault  
Adviser

Dr. Eric Weeks

Committee Member

Dr. William G. Kelly

Committee Member

Dr. Gordon Berman

Committee Member

2017

Investigating *in utero* Fertilization, *in vitro* Fertilization, and the Mermaid-2 Voltage Sensor in  
*Caenorhabditis elegans*

By

Hugh W. Phillis

Dr. Steven L'Hernault

Adviser

An abstract of  
a thesis submitted to the Faculty of Emory College of Arts and Sciences  
of Emory University in partial fulfillment  
of the requirements of the degree of  
Bachelor of Arts with Honors

Department of Physics

2017

## Abstract

Investigating *in utero* fertilization, *in vitro* fertilization, and the Mermaid-2 Voltage Sensor in *C. elegans*

By Hugh W. Phillis

*C. elegans* share a genetic homology with humans and thus may provide valuable insights into human biology, chemistry, and more. The L'Hernault lab identifies and investigates fertilization defective mutant strains of *C. elegans*. The *spe-9* class mutants are of interest because they produce seemingly normal spermatozoa, but are unable to fertilize an oocyte. However, tools need to be developed to further study, evaluate, and classify these mutants. My objectives were to induce and document *in utero* fertilization, develop a protocol for *in vitro* fertilization, and create a voltage sensor to investigate ion shifts during fertilization. I have gathered a substantial amount of evidence proving *in utero* fertilization of nonEmo oocytes can occur. Normally, fertilization occurs in the spermatheca and no prior work has found it to occur elsewhere in *C. elegans*. One reason is that wild-type oocytes complete meiosis upon entering the spermatheca and undergo endomitosis (Emo) if they fail to be fertilized. Prior work has shown that the *pezo-1* mutant forms oocytes that remain in meiosis, even if they are not fertilized. These nonEmo oocytes were evaluated in my work to explore if they could be fertilized outside of the spermatheca. This suggests that the mutant nonEmo oocyte phenotype maintains fertilization competency after passing through the spermatheca. In addition, it also suggests that spermatozoa do not undergo any special capacitation event within the spermatheca. Most importantly, it signifies that *in vitro* fertilization might be possible. However, *in vitro* fertilization has yet to be realized. Lastly, I have successfully created a plasmid containing the Mermaid-2 voltage sensor and have used transgenic techniques to induce its expression in the germline of *C. elegans*. Future research must center on utilizing the Mermaid-2 voltage sensor to evaluate fertilization defective mutants and successfully completing *in vitro* fertilization. These efforts may one day reveal new insights in to mammalian fertilization and be used in the treatment of infertility.

Investigating *in utero* Fertilization, *in vitro* Fertilization, and the Mermaid-2 Voltage Sensor in  
*Caenorhabditis elegans*

By

Hugh W. Phillis

Dr. Steven L'Hernault

Adviser

A thesis submitted to the Faculty of Emory College of Arts and Sciences  
of Emory University in partial fulfillment  
of the requirements of the degree of  
Bachelor of Arts with Honors

Department of Physics

2017

## Acknowledgements

I would like to thank Dr. Steven L'Hernault for giving me the opportunity to perform research in his lab over the past two years. His guidance and mentorship have helped me grow and develop as a student and researcher. In addition, I am enormously grateful for Elizabeth Gleason and Dr. Huiping Ling for their help, patience, and insight during my research. I would also like to thank my committee members, Dr. Eric Weeks, Dr. Gordon Berman, and Dr. William Kelly, for their valuable insights and assistance. Lastly, I want to specifically thank Dr. L'Hernault and Dr. Weeks for collaborating between their departments to allow a physics major to complete an Honors Thesis with biology research.

I would also like to thank my parents, family, and friends for their continuous support throughout my education and research. I would particularly like to thank my sister, Stevie Phillis, for introducing me to Dr. L'Hernault and his lab in 2013.

## Table of Contents

|   |      |
|---|------|
| <b>Chapter I: Introduction</b>  | (1)  |
| A. Overview of <i>Caenorhabditis elegans</i> ( <i>C. elegans</i> )    | (1)  |
| B. Hermaphroditic Reproductive Anatomy                                | (2)  |
| C. Male Reproductive Anatomy  | (2)  |
| D. Fertilization in <i>C. elegans</i>                                 | (3)  |
| <b>Chapter II: <i>in utero</i> Fertilization (IUF)</b>                | (7)  |
| A. Introduction   | (7)  |
| B. Materials and Methods  | (7)  |
| C. Results  | (10) |
| D. Discussion   | (12) |
| <b>Chapter III: <i>in vitro</i> Fertilization (IVF)</b>               | (15) |
| A. Introduction   | (15) |
| B. Materials and Methods  | (17) |
| C. Results  | (22) |
| D. Discussion   | (24) |
| <b>Chapter IV: Creating Mermaid-2 Expression in <i>C. elegans</i></b> | (26) |
| A. Introduction   | (26) |
| B. Materials and Methods  | (29) |
| C. Results  | (31) |
| D. Discussion   | (32) |
| <b>Chapter V: Future Directions</b>                                   | (34) |
| <b>Figures and Tables</b>   | (36) |
| <b>References</b>   | (70) |

## Chapter I: Introduction

### A.) Overview of *Caenorhabditis elegans* (*C. elegans*)

In the mid-twentieth century, Sydney Brenner developed the nematode *Caenorhabditis elegans* (*C. elegans*) as a model genetic organism. Since Brenner's novel discovery, over 7,000 articles have been published investigating this organism. The emergence of the *C. elegans* as a superior model organism is due to numerous reasons. For example, they are microscopic, transparent, exhibit sexual dimorphism, are inexpensive to cultivate, have a quick life cycle, and their entire genome is sequenced. In addition, there is 40% homology between the *C. elegans* and human genomes. Therefore, humans and *C. elegans* share a common ancestor and studying *C. elegans* could provide insights into human biology, chemistry, and more. In sum, these characteristics distinguish *C. elegans* as an ideal model for genetic analysis [1].

The *C. elegans* life cycle can be divided into seven stages: embryonic development, four larval phases, adulthood, and senescence preceding death. [2] However, an additional phase characterized by arrested development can appear during the second larval phase (L2) if environmental stresses such as unfavorable temperature, population density, or a lack of food occur. This is known as the dauer phase [3]. Moreover, temperature cannot only instigate the emergence of a dauer phase, but it can also impact developmental rates. At 15 °C, the development from an embryo to a reproducing adult takes 90 hours [2]. At 20 °C, the complete life cycle takes 54 hours [1]. At 25 °C, this same development occurs in 45 hours [2]. Once adulthood is reached, the hermaphroditic worm will self-fertilize its oocytes and lay embryos for two to three days. After this, the worm may continue living for several weeks until senescent death [1].

In contrast to human somatic cells, which contain 23 pairs of chromosomes, *C. elegans* cells possess only 6 pairs of chromosomes. Moreover, chromosomes one through five are autosomal and the sixth is a sex chromosome. This nomenclature is analogous in humans. The first 22 chromosomes are autosomal and the final pair are the sex chromosomes, XX or XY. In *C. elegans*, the presence of two X chromosomes (XX) results in hermaphrodites, while one X chromosome (X0) is observed in male lines [1, 4]. Although this sexual dimorphism exists, wild-type *C. elegans* populations are composed predominately of hermaphrodites [1]. Males only make up 0.1% of the natural population, and arise due to nondisjunction of the X chromosome [5]. However, many mutant lines that regularly produce elevated numbers of males are now known. The general anatomy and reproductive system of males exhibit distinct differences when compared to hermaphrodites [1].

#### *B.) Hermaphroditic Reproductive Anatomy*

In hermaphrodites, there is a two-armed bilaterally symmetric gonadal structure. Each gonad arm can be separated into four regions: the proximal gonad, distal arm, spermatheca, and uterus. The proximal gonad, spermatheca and uterus can be equated to the mammalian ovary, oviduct, and uterus, respectively [6]. Figure 1A displays an anatomical diagram of a hermaphrodite.

#### *C.) Male Reproductive Anatomy*

Male *C. elegans* have several key anatomical differences from hermaphrodites. First, a fan-like tail is a distinctive feature of males. Additionally, this tail has spicules that aid in mating. Second, males possess a single gonadal arm. Spermatogenesis produces spermatids that are stored in seminal vesicles until they are ejaculated into a hermaphrodite's uterus

during copulation [7]. These spermatids activate to become motile spermatozoa when they enter the uterus. Figure 1B displays an anatomical diagram of a male *C. elegans*.

#### *D.) Fertilization in C. elegans*

##### *i. Spermatogenesis*

Spermatogenesis is the process by which undifferentiated germ cells develop into spermatozoa. First, spermatogonia mitotically divide to produce primary spermatocytes. Simultaneously, a central cytoplasmic core is formed termed the rachis. The primary spermatocyte then undergoes DNA replication developing from 2N to 4N [8]. Primary spermatocytes then enter meiosis I and divide into two 2N cells called secondary spermatocytes [7]. When this division occurs, the secondary spermatocytes either completely separate or remain attached [8]. Meiosis II immediately follows and produces four haploid spermatids. The spermatids bud off from the residual body and selectively contain the nucleus, mitochondria, and lysosome-like organelles called fibrous body-membranous organelles (FB-MOs). The ribosomes, voltage-gated ion channels, tubulin, and actin are all segregated into the residual body. Eventually, spermatids develop further, transforming into spermatozoa. This transformation, called spermiogenesis, results in several physiological changes. Two of the most notable are the fusion of MO's to the cell body's surface and the formation of a pseudopod [7]. Figure 2 provides a visual overview of the development of primary spermatocytes to spermatozoa. It is important to note that spermiogenesis, the transition to activated spermatozoa, can also occur *in vitro* using the protease Pronase, ionophore monensin, weak bases, calmodulin inhibitors, the ion channel inhibitor DIDS, or media

containing zinc [7-9]. Mature *C. elegans* spermatozoa do not possess an acrosome or flagella. They are motile solely due to a pseudopod [7].

There are several key differences between male and hermaphroditic sperm production. First, hermaphrodites initiate spermatogenesis during the fourth larval (L4) phase. After this, they switch to oogenesis [8]. Second, spermiogenesis is initiated in hermaphrodites when an oocyte pushes spermatids into the spermatheca during ovulation. Conversely, spermiogenesis is initiated in males when spermatids are mixed with seminal fluid and ejaculated into a hermaphrodite's uterus [7].

## *ii. Oogenesis and Fertilization*

Hermaphrodites shift from spermatogenesis to oogenesis as they transition from L4's to adults [6]. Oocytes move from the distal to proximal gonadal arms as they develop and eventually arrest after diakinesis, which is the final stage of meiosis I prophase. As the oocyte traverses the proximal gonadal arm or oviduct, it eventually reaches the spermatheca [10]. The first ovulation pushes spermatids into the spermathecal, where they develop into spermatozoa. These spermatozoa self-fertilize oocytes as they travel through the spermatheca to the uterus [7]. Finally, embryos in the uterus will be expelled to the exterior through the vulva. Figure 3 provides an overview of oogenesis and self-fertilization in hermaphrodites.

Fertilization can also occur after a male mates with a hermaphrodite. After a male has inseminated a hermaphrodite, the sperm crawl into the spermatheca and outcompete hermaphrodite-derived sperm to fertilize the oocyte. The male-derived sperm will fertilize virtually all of the oocytes until the only sperm left are those from the hermaphrodite. This results in a near complete suppression of hermaphroditic self-fertilization and an outcross of

genes [11]. This phenomenon is exemplified in Figure 4. Additionally, certain male *C. elegans* strains deposit copulatory plugs over the hermaphrodite's vulva to inhibit re-mating, prevent sperm from being expelled from the uterus, and increase the number of cross-progeny [12].

If for some reason an oocyte passes through the spermatheca and is not fertilized, the nucleus exits meiosis and undergoes mitosis, developing into a defective oocyte with a polyploid nucleus. This resulting phenotype is referred to as endomitotic (Emo). However, strains have been discovered where this mitotic transition does not occur, resulting in a nonEmo phenotype. In these strains, the oocytes remain meiotically arrested. The *C10C5.1/pezo-1* gene results in the nonEmo phenotype without affecting the competence of oocytes to be fertilized [13].

#### *E. Similarities and Differences between Human and C. elegans Reproduction*

Humans, along with all other mammals, reproduce sexually. In other words, male-derived sperm and a female-derived oocyte combine to form a diploid embryo [14]. As previously stated, this can also occur between males and hermaphrodites in *C. elegans*. Although differences between human and *C. elegans* reproductive anatomy are dramatic, there are some similarities. For instance, both species exhibit bilateral symmetry in their reproductive organs [13]. In addition, the proximal gonad arm, spermatheca, and uterus in *C. elegans* is analogous to the human ovary, oviduct, and uterus, respectively [6]. In both species oocytes are arrested at the final stage of prophase I before ovulation [10].

Some of the most obvious reproductive differences between humans and *C. elegans* regard germ cells. In contrast to *C. elegans*, which undergo oogenesis after spermatogenesis, female humans are born with a fixed number of oocytes [15]. These oocytes are meiotically

arrested at prophase I and are enveloped by primordial follicles. In a coordinated fashion, the pituitary, hypothalamus, and ovary hormonally regulate the ovarian, uterine, and cervical cycles. For example, after a surge in follicle stimulating hormone (FSH) to drive oocyte development, a rise in leutinizing hormone (LH) restarts meiosis until it is again arrested at metaphase II of meiosis II [16, 17]. On average, oocytes are ovulated every 29.5 days in what is known as the menstrual cycle [16]. Meiosis will only resume and be completed after fertilization. If fertilization does not occur, the uterine lining and oocyte will be shed [17]. In the absence of fertilization, the second meiotic arrest in humans differs sharply from the endomitotic replication observed in *C. elegans*.

Male germ cells also differ greatly between the two species regarding origin, anatomy, and function. In healthy adult male humans, spermatozoa are continuously produced at a rate of one thousand per second [15]. Spermatogenesis occurs in *C. elegans* hermaphrodites only during the L4 stage before switching to oogenesis [8]. Furthermore, in hermaphrodites, spermatozoa competent for fertilization are only formed after the first ovulation. They do not possess a flagella or acrosome, as seen in human sperm [6]. In humans, spermatozoa are not competent to fertilize an oocyte until capacitation and the acrosome reaction occur. Capacitation occurs in the female reproductive tract and involves physiological changes to the head, acrosome, and flagella to aid in fertilization. The acrosome reaction involves the sperm binding to the zona pellucida (ZP) of the oocyte [14, 15]. The acrosome reaction in mammals is roughly equivalent to the MO fusion in *C. elegans* [18].

## Chapter II: *in utero* Fertilization

### A.) Introduction

Normally, *C. elegans* fertilization only occurs in the spermatheca. In order for fertilization to occur, an oocyte arrested at diakinesis must interact with a spermatozoon as it is being squeezed into the spermatheca [13]. As stated previously, *pezo-1* (nonEmo) mutants result in meiotically arrested oocytes *in utero* after expulsion from the spermatheca into the uterus. Additionally, spermiogenesis of male-derived spermatids occurs after they are mixed with seminal fluid and are ejaculated into the hermaphrodite's uterus. However, the mechanism that activates spermiogenesis *in vivo* is not fully understood [7]. If an oocyte is fertilized *in utero*, this would reveal that the spermatheca is not essential in activating the spermatozoa. It would also demonstrate the nonEmo oocytes that have travelled through the spermatheca retain fertilization competence *in utero*. Lastly, successful *in utero* fertilization would suggest that *in vitro* fertilization is possible, using the *pezo-1* mutant as the oocyte donor strain.

### B.) Materials and Methods

#### i. Mutant Strains

Four hermaphroditic and three male strains were used to investigate the feasibility of *in utero* fertilization (IUF; Table 5). Every hermaphroditic line exhibited a nonEmo phenotype and was also self-sterile at 25°C. One hermaphroditic strain used was SL1651. This line has a green plasma membrane in oocytes and red DNA fluorescence. Another hermaphroditic strain used, SL1655, has only red DNA fluorescence. Similarly, SL1698 was utilized and it expressed red DNA fluorescence. Finally, SL1607 was utilized, and it did not have any fluorescent markers. These

strains were deliberately chosen for their phenotypic characteristics. The suppression of self-fertility at 25°C is critical to ensure that oocytes will be ovulated but not fertilized. SL1607, SL1651, and SL1655 all suppress self-fertility via *fer-1(b232ts)* while SL1698 has *spe-9(hc88ts)*. Moreover, the induction of the nonEmo phenotype in *pezo-1(ebDf1)* results in meiotically arrested oocytes potentially competent for *in utero* fertilization. Lastly, fluorescent markers (*itIs37*, *itIs38*) aid in observing any embryonic changes or developments.

As stated, three male lines were also used to investigate IUF: CB4855, SL1352, and SL1699 (Table 5). CB4855 is a wild strain that has better male mating ability (~90%) as compared to Bristol N2 (~60%) [19]. Additionally, copulatory plugs form over the vulva after mating to CB4855 males because they are *plg-1(e2001)* [19]. Another male line, SL1352, has green fluorescent nuclei (*zuls178*), but it does not induce copulatory plugs. The final male line used was SL1699. It has a red pharynx (*hjsi20*) and forms copulatory plugs because it is *plg-1(e2001)*. The fluorescent markers in SL1352 and SL1699 enable the simple determination of paternity of any male-derived progeny.

### *ii. Culture and Mating Conditions*

*C. elegans* were cultivated on NGM plates with OP50 *E. coli* bacteria as a food source. [20] Hermaphroditic lines were either incubated at 16°C or 25°C, but were only self-fertile at 16°C. All male lines were stored at 20°C.

### *iii. in utero Fertilization Trials*

The first phase of IUF trials utilized SL1352 male worms. SL1651 and SL1655 were utilized as self-sterile hermaphroditic lines. These hermaphroditic lines exhibited red fluorescent markers in their nuclei and displayed clear distinctions between Emo and nonEmo

oocytes as well as between oocytes and embryos. First, embryos and L1's from the hermaphroditic lines were transferred onto a new plate and incubated at 25°C to allow growth and inhibit self-fertilization. Approximately 24 hours later, 60-80 males were isolated onto one plate and incubated at 20°C. After the hermaphroditic worms were grown for 46-48 hours, they were transferred onto individual, single-spotted plates. Four males were then transferred onto each plate. In total, 15-20 mate plates were set up per experiment. All plates were observed every 10 minutes to see if a copulatory plug was evident over the vulva of the hermaphrodite, indicating a successful mating had occurred [12]. Once a mate was confirmed by the presence of a copulatory plug, the hermaphrodite was transferred into a 0.2 mM levamisol solution on a slide. The slide was examined using differential interference contrast (DIC) microscopy via a compound microscope. Epifluorescence was also observed using a Texas Red (TR) filter on the same microscope to check for the fertilization and subsequent development of any embryos *in utero*.

In phase two of *in utero* trials, mates were set up only using CB4855 males and SL1655 hermaphrodites. These changes occurred because of the emergence of Emo oocytes in SL1651 hermaphrodites and the lack of observable green fluorescence in SL1352. Additionally, instead of individual mate plates, 15-20 hermaphrodites were transferred onto a plate with approximately 60 males. This final change enabled a more efficient observation of mating and detection of copulatory plugs.

The third phase utilized two lines: SL1699 and SL1698 hermaphrodites. The male line was picked so that any paternal progeny could easily be identified by the presence of a red pharynx. Additionally, the hermaphroditic mutant was chosen because it did not exhibit oocyte

crowding *in utero*. Hermaphrodites and males were incubated using identical methods as in previous trials. As in the second phase, 15-20 hermaphrodites were transferred onto a plate with approximately 60 males. Once a successful mating was confirmed by the presence of the copulatory plug over the vulva, the hermaphrodite was suspended in a 0.2 mM levamisol solution on top of a 5% agar pad. The slide was then examined using DIC microscopy and a TR filter on a compound microscope.

The final phase of trials utilized SL1607 hermaphrodites and SL1699 males. Like previous trials, the male line was chosen so that paternal progeny could be easily identified. An identical protocol was used to incubate and mate males and hermaphrodites. However, after a mate was confirmed by the presence of a copulatory plug, the hermaphrodite was moved onto a separate plate and observed using a dissecting microscope, Olympus SXZ12. Then, pictures were taken as embryos and/or oocytes were laid onto an agar plate. After approximately eight embryos or oocytes were laid, the adult hermaphrodite was transferred onto a fresh plate.

### *C.) Results*

The first phase of *in utero* trials yielded indirect evidence of fertilization occurring outside of the spermatheca. No oocytes were directly observed transitioning to an embryo, however there was evidence of fertilization of oocytes in the uterus. Figure 6 shows the presence of embryos near to the vulva with oocytes lined up distally to the spermatheca. This suggests that the oocytes were not fertilized within the spermatheca but in the uterus after insemination from the male. In a different trial, an embryo was observed in between oocytes in the uterus within three hours of mating (Figure 7). Similar logic suggests fertilization outside of the spermatheca, and both results were observed in SL1651 hermaphrodites.

The second phase of *in utero* trials also provided evidence of fertilization occurring outside of the spermatheca. Immediately after a copulatory plug was observed, the hermaphrodite was analyzed using DIC microscopy and a TR filter. A four-celled embryo was documented directly next to the vulva. About one hour later, the embryo had developed into a sixteen-cell embryo (Figure 8). After 24 hours, it had hatched within the hermaphrodite, producing live progeny. The paternity of the progeny was not confirmed.

In the third phase of IUF trials, an embryo was observed undergoing its first divisions *in utero*. A four-celled embryo was observed close to the vulva, however there were no obvious oocytes lined up behind it (Figure 9). The change in hermaphroditic lines is solely due to observed retention of oocytes *in utero* in SL1655. We believed that the resulting crowding of oocytes *in utero* acted as a physical block to the ejaculate. SL1699 males succeeded CB4885 males because they exhibited a red pharynx. The embryo formed in Figure 9 possessed this fluorescent phenotype.

In the final phase of trials, early-stage embryos were observed being laid. After two oocytes were laid, an embryo was laid onto the agar plate and observed in the early stages of development. Sperm and oocyte pronuclei were observed as separate entities (Figure 10A, B) that fuse minutes later (Figure 10C, D). Then, the first cleavage occurred forming a two-celled embryo (Figure 10E). Two other embryos were also laid, but one was dead, before the adult was transferred to a new plate. The paternity of the resulting progeny was then confirmed because it had a red pharynx, which is a trait conferred by the male genotype (Figure 11). In addition, a two-celled (Figure 12A) and two four-celled embryos (Figure 12B) were laid from a different hermaphrodite. It is important to note that no oocytes were laid, and five of the eight

embryos hatched. The paternity was also confirmed by the presence of a red pharynx in all five that hatched (data not shown). Lastly, approximately 40% of mated hermaphrodites laid immature embryos between 1-8 cells.

#### *D.) Discussion*

In wild-type worms, oocytes are fertilized as they are squeezed through the spermatheca. In all observed cases, the first spermatozoa to interact with an oocyte in the spermatheca immediately fertilize it [21]. Embryos then enter the uterus and continue to divide and mature as they move towards the vulva. Each embryo is approximately 30 cells when it is expelled through the vulva to the exterior [1]. Therefore, a distinct pattern occurs in the uterus in which the latest stage embryos are closest to the vulva.

In addition, the timing of embryonic development is critical in assessing when and where an oocyte was fertilized. After copulation, male-derived sperm reach the spermatheca in about one hour [21]. Then, within five minutes of fertilization, the sperm and oocyte pronuclei fuse [22]. This occurs either in the spermatheca or in the uterus near the spermatheca. Then, the embryo's journey from the spermatheca to the vulva takes roughly two hours, and results in several cleavages forming a 30-cell embryo [1, 23].

In phases one and two of the IUF trials, embryos were observed *in utero* either in between oocytes or with only oocytes distal to them (Figures 6, 7). If fertilization is occurring in the spermatheca, one would expect to see embryos distal to any oocytes. One might argue that these patterns emerged because a small number of sperm reached the spermatheca and participated in fertilization. However, the large number of ejaculated sperm and high fertilization rate of sperm at the spermatheca make the prospect of the fertilization at the

spermatheca very unlikely [21]. Based on my results (Figures 5, 6), the most probable explanation is that fertilization occurred outside of the spermatheca in the uterus.

Additionally, in phases two and three of the IUF trials, four-celled embryos were observed proximal to the vulva (Figures 8, 9). This stands in stark contrast to what embryos at a similar location look like in wild-type *C. elegans* as well as in self-fertilizing versions of these experimental mutants (Figure 13). As stated previously, the timing of embryonic development relative to location is critical to determining where an oocyte was fertilized. In a phase 3 trial, a newly shelled embryo is initially seen and documented *in utero* (Figure 9A, 9B), and 57 minutes later, it is a four-celled embryo is observed directly behind the vulva (Figure 9C, 9D). This is highly suggestive of *in utero* fertilization since it would have taken an hour for the sperm to reach the spermatheca plus another 30 and 40 minutes to develop into a four-celled embryo after fertilization [22]. Thus, these trials provide evidence of fertilization occurring outside of the spermatheca, specifically *in utero*.

Lastly, I witnessed and documented embryos being laid within minutes of fertilization. For example, I witnessed the fusion of male and hermaphroditic nuclei after the embryo exited the uterus through the vulva. Again, this fusion of pronuclei normally occurs within five minutes of fertilization either in the spermatheca or in the uterus near the spermatheca [22]. In addition, I witnessed multiple instances where 2 and 4 celled embryos were being laid (Figure 12). These cleavages normally occur about 12 and 28 minutes after fertilization, respectively, in the uterus, hours before the embryo is laid [22]. In wild-type worms, it takes approximately three hours for sperm to travel to the spermatheca, fertilize an embryo, and the embryo to be expelled from the uterus. Over this time, the embryo will normally develop into a 30-cell

embryo before it is laid [1, 21, 23]. I confirmed that this fertilization defective mutant behaves similarly by incubating self-fertilizing adults at 25°C for one hour and then allowing them to lay embryos. All embryos observed were far more mature than those observed in the IUF trial, and closely resembled normal embryonic development in wild-type *C. elegans* (Figure 14).

Therefore, the fact that laid embryos observed in the IUF trial were in a much earlier in developmental stage leads to several deductions. First, the embryos did not spend as much time *in utero* and thus did not undergo as many divisions. Second, the oocytes must have been fertilized in the uterus, close to the vulva and distant from the spermatheca.

Moreover, one of the worms I evaluated should have been self-sterile but did not lay any oocytes despite having oocytes in the uterus prior to mating. Red pharynxes proving cross-progeny were observed in all hatched embryos. The most likely explanation is that *in utero* oocytes were fertilized. Roughly 40% of the mated hermaphrodites laid embryos that were at an earlier than normal developmental stage. This may indicate that it is common for nonEmo oocytes to retain fertilization competency, strongly supporting the potential for IVF.

There is strong evidence that IUF occurred in these trials. Several important considerations should be drawn including that nonEmo oocytes maintain their fertilization competency after passing through the spermatheca. This is immensely important because these self-sterile hermaphrodites are the only known source of competent oocytes for *in vitro* fertilization (IVF). Second, IUF suggests that spermatozoa do not undergo any special ‘capacitation’ within the spermatheca [24]. Although some ‘capacitation’ event might occur *in vivo*, it is also possible that spermatozoa are inherently competent to fertilize oocytes. Thus, these results suggest that activated male sperm are capable of IVF.

## Chapter III: IVF

### A.) Introduction

In 1959, M.C. Chang completed the first successful mammalian IVF in rabbits [25]. Ejaculated sperm were harvested *in utero* post-copulation and combined with recently ovulated oocytes in solution. The IVF media closely mirrored *in vivo* conditions regarding pH, temperature, and chemical composition. Since then, numerous mammalian species have undergone successful IVF, including mice, rats, guinea pigs, cows, pigs, and, of course, humans [26].

In the mid-twentieth century, human IVF was pioneered by Dr. Robert Edwards, with the assistance of Dr. Patrick Steptoe and Dr. Barry Bavister. Their crucial breakthrough occurred in the late 1960's when they were able to induce human sperm capacitation *in vitro*. Oocytes were acquired through ovarian biopsy and then developed *in vitro*. They then combined fertilization-competent sperm and mature oocytes, in what is known as Bavister's Solution, and produced human embryos [24]. Edward's ultimate success occurred in 1978 when Louise Brown was born, the world's first IVF baby. Since then, over five million people have been conceived using IVF techniques [27].

While human IVF has principally been used to remedy infertility, IVF in *C. elegans* offers different potential benefits. Most obviously, IVF would enable the unobscured observation of spermatozoa-oocyte interactions and the fertilization process. It would also reveal temporal, spatial, and environmental influences on fertilization. IVF would also aid in the differentiation and understanding of various *spe-9* class mutants, which are thought to specifically affect fertilization [6]. Lastly, it would also be valuable in the evaluation of fertility drugs [13].

However, IVF in *C. elegans* has yet to be realized because of three main challenges. The first challenge is finding a viable source of nonEmo oocytes. The second obstacle is inducing spermiogenesis and creating fertilization-competent spermatozoa. The final challenge is to produce a media compatible with both oocytes and spermatozoa in which fertilization can occur.

A step towards solving the first challenge was taken in 1997 when McCarter et al. published their findings on *him-8(e1462)* mutants. They found that fertilization-defective hermaphrodites in this mutant line possessed *in utero* oocytes arrested in diakinesis of prophase I of meiosis I [28]. In contrast to wild-type phenotypes, unfertilized oocytes did not endomitotically replicate after ovulation. This phenotype was characterized as nonEmo. The work of K. Pohl, C. Elam, E. Gleason, and S. W. L'Hernault confirmed that the gene C10C5.1 on chromosome IV produced this phenotype [13, 29]. My work in Chapter I showed that these oocytes remain competent to be fertilized *in utero*.

The second obstacle to *C. elegans* IVF has also been tackled. Several ways to activate sperm *in vitro* have been discovered. Spermiogenesis can be initiated via the cationic ionophore monensin [30]. Sperm can also be activated by proteases, but Pronase induced activation does not result in fertilization competent spermatozoa. Conversely, sperm activated with triethanolamine (TEA) are fertilization competent [31, 32]. Sperm can be activated with a phosphoinositide 3-kinase inhibitor wortmannin [6, 33]. Lastly, zinc can be used to activated spermatids [9].

The final hurdle to IVF is creating a suitable media in which fertilization can occur. However, no IVF media has been established to this date. One may assume that the media

must roughly mirror the pH, osmolarity, and chemical composition of *C. elegans* reproductive tract *in vivo*. Moreover, although no IVF media has yet been synthesized, known solutions are compatible with sperm or embryos, but not both. For example, embryo buffer (118 mM NaCl, 48 mM KCl, 2 mM CaCl<sub>2</sub> 2H<sub>2</sub>O, 2 mM MgCl<sub>2</sub> 6H<sub>2</sub>O, and 25 mM HEPES; pH 7.3) has been extensively used to study embryonic development after shell removal *in vitro* [34]. Similarly, 1X Sperm Media (50 mM HEPES, 25 mM KCl, 45 mM NaCl, 1 mM MgSO<sub>4</sub>, 5 mM CaCl<sub>2</sub>, 10 mM dextrose; pH 7.0 or 7.8) is compatible with sperm and is optimal for their *in vitro* observation [30, 35]. One of the principle differences between these solutions is osmolarity. 1X Sperm Media and egg buffer have osmolarities of 240 mOsm and 340 mOsm, respectively. Furthermore, it is known that cultured *C. elegans* cells are sensitive to osmotic pressure [36]. Thus, although oocytes appear healthy in egg buffer, deviations in osmolarity from 340 mOsm may result in significant morphological changes and deformations. This is an important consideration in deriving an IVF media as the ideal sperm solution has a much lower osmolarity.

## *B.) Materials and Methods*

### *i. Mutant Strains*

Three male *C. elegans* lines and two hermaphroditic *C. elegans* lines were employed during IVF trials; CB4855, AV285, and SL1699 (Table 5). CB4855 is a wild strain that has better male mating ability as compared to Bristol N2 [19]. It also has extra-large sperm, a higher number of progeny, and ultra-competitive sperm [1]. Additionally, copulatory plugs form over the vulva after mating because it is *p/g-1(e2001)* [19]. Lastly, it transfers sperm in 90% of its mates. Another male line used was SL1699. It has a red pharynx (*hjsi20*) and forms copulatory plugs because it is *p/g-1(e2001)*. The presence of this phenotype easily identifies any male-

derived progeny. The final male line used was AV285. This line is distinctive in that it contains activated spermatozoa *in vivo* because inhibition of activation does not occur [37].

The hermaphroditic lines utilized were SL1607 and SL1698 (Table 4). Both hermaphroditic lines exhibited temperature sensitive self-fertility and the nonEmo phenotype, but only the latter possessed red fluorescence via a histone marker which aided in microscopic observation.

### *ii. Culture Conditions*

*C. elegans* were cultivated on NGM plates with OP50 *E. coli* bacteria as a food source [20]. Hermaphroditic lines were either incubated at 16°C or 25°C, but were only self-fertile at 16°C. All male lines were grown at 20 °C.

### *iii. Solutions*

A variety of media were utilized during IVF trials. 1X Sperm Media, egg buffer, worm homogenate, Shelton's Media, and synthetic porcine mucus were either used separately or in combination to create a suitable media in which IVF could potentially occur [38].

1X Sperm Media consists of 50 mM HEPES, 25mM KCL, 45 mM NaCl, 1 mM MgSO<sub>4</sub>, 5mM CaCl<sub>2</sub>, and 10 mM dextrose, at a pH of either 7.0 or 7.8. In addition, the osmolarity should be 240 mOsm [39]. Osmolality was measured to be 240 mMol/kg using the VAPRO Vapor Pressure Osmometer. During each experimental trial, I made fresh 1X working sperm media by combining 158.2 μl H<sub>2</sub>O, 40 μl 5X sperm media, and 1.8 μl 20% dextrose.

Egg buffer is composed of 118 mM NaCl, 48 mM KCl, 2 mM CaCl<sub>2</sub> 2H<sub>2</sub>O, 2 mM MgCl<sub>2</sub> 6H<sub>2</sub>O, and 25mM HEPES [34]. The pH is adjusted to 7.3, and the osmolarity was 365 mOsm (osmolality = 365 mMol/kg).

Worm homogenate was created via a protocol from Dr. Long Miao at the Institute of Biophysics, Chinese Academy of Science, Beijing. Wild-type worms (N2) were grown in liquid culture and then spun down in a solution of 1X Sperm Media with PVP (10 mg/ml) instead of dextrose. The resulting solution was decanted and the supernatant is discarded, leaving the pellet of worms. This pellet was homogenized by one of two methods. It is either homogenized in a French press or frozen under liquid nitrogen and then ground into a powder using a pestle and mortar. The products were then subjected to centrifugation at 21,130 relative centrifugal force (rcf) to separate the liquid phase. The resulting worm homogenate was boiled for one minute, centrifuged again (21130 rcf), and passed through an ultrafiltration device to remove molecules  $\geq 10000$  MW. Worm grind, created using liquid nitrogen and subsequent grinding, had a pH of 6.5 and a molality of 280 mMol/kg. In contrast, worm squash, created using the French press, had a pH of 6.5 and molality of 485 mMol/kg.

Synthetic porcine mucin was also evaluated. Mucin was a 100 mL solution containing 1 g guar gum, 0.5 g dried porcine mucin, 0.3 g imidurea, 0.15 g methylparaben, 0.02 g propylparaben, 0.26 g dibasic  $K_2HPO_4$ , 1.57 g monobasic  $K_2HPO_4$ , 96.2 g  $H_2O$ , and 1 mL of 0.1M  $Na_2B_4O_7 \cdot 10H_2O$  [40].

Lastly, Shelton's Medium was prepared according to a published protocol [38]. First, a 5 mg/ml inulin solution was autoclaved. Then, 1 ml of 5 mg/ml inulin, 50 mg PVP powder, 100  $\mu$ l BME Vitamins, 100  $\mu$ l lipid concentrate, 100  $\mu$ l penicillin-streptomycin, and 9 ml of *Drosophila* Schneiders' Medium were combined. Lastly, before each trial fetal calf serum (FCS) was added to an aliquot of the preceding solution to create an overall 35% FCS solution [38]. The resulting solution had an osmolality of 280 mMol/kg and pH of 7.25.

#### *iv. Methods*

Although I utilized a wide range of solutions during IVF trials, they all follow a general protocol. I first transferred embryos and L1's to a spotted plate at 25°C and allowed them to mature into self-sterile adults. Males were usually isolated and incubated at 20°C either on the same day or a day after hermaphrodites were shifted to 25°C. The isolation of male *C. elegans* maximized the number of sperm stored in the seminal vesicle. After the hermaphrodites had been incubated for 48-60 hours, males were transferred into an 8 µl solution on a glass slide. The male worms were then dissected, severing the gonad and releasing sperm into solution. This was accomplished by hand using 30G BD PrecisionGlide Needles. After 15 minutes of activating sperm in solution, hermaphrodites were dissected to release oocytes into solution. After adding a cover slip, the oocytes and sperm were then analyzed using DIC microscopy.

The first phase of IVF experiments exactly mirrored the general protocol outlined above. It involved SL1607 hermaphrodites and two male lines, AV285 and CB4855. Only one male line was dissected per slide well, and 1X Sperm Media pH 7.0 was utilized for all trials.

The second phase of IVF experiments utilized a solution based in egg buffer, 20% dextrose, ZnCl<sub>2</sub> (.05 M), polyvinylpyrrolidone (PVP; 100 mg/ml), and protease-free Bovine Serum Albumin (BSA; 10 mg/ml). PVP and BSA were used separately to make two distinct solutions. The first consisted of 195.2 µl egg buffer, 2 µl ZnCl<sub>2</sub>, 1.8 µl 20% dextrose, and 1 µl PVP. The second consisted of 186.2 µl egg buffer, 2 µl ZnCl<sub>2</sub>, 1.8 µl 20% dextrose, and 10 µl BSA. In addition, solutions were synthesized with varying ratios of these two solutions. Identical worm strains were used and all other procedures were followed as before.

The third phase of IVF trials combined the two previous stages. The IVF solution now consisted of 156.2  $\mu\text{l}$  egg buffer, 40  $\mu\text{l}$  5X Sperm Media, 2  $\mu\text{l}$   $\text{ZnCl}_2$  (.05 M), and 1.8  $\mu\text{l}$  20% dextrose. One important note is that only CB4855 males were used in this phase. However, all other procedures occurred as before.

I tried to replicate the conditions inside the *C. elegans*' reproductive tract during the fourth phase of IVF experiments by utilizing synthetic porcine mucin. Once created, the mucin was dried on a slide. Identical procedures and solutions were then used in conjunction with the mucin coated slides.

Many changes occurred with the advent of the fifth phase of IVF trials. The male line, CB4855, was now first dissected in a solution of 3.5  $\mu\text{l}$  1X Sperm Media, 1  $\mu\text{l}$  worm homogenate, and either 2 or 4  $\mu\text{l}$  of  $\text{ZnCl}_2$  (.05 M). After dissection and the release of sperm into solution, the slides were placed in a humid chamber for 15 minutes. Next, I added 3.5  $\mu\text{l}$  of egg buffer solution (198  $\mu\text{l}$  egg buffer, 2  $\mu\text{l}$  20% dextrose) was added to the solution, followed by SL1607 hermaphrodites. nonEmo oocytes were then dissected from the hermaphrodites and mixed with the sperm in solution.

The final phase of IVF trials mirrored the fifth phase in procedure, but utilized different strains and solutions. In this phase, SL1699, SL1698, and SL1607 strains were used (Table 5). Males were first dissected in 6  $\mu\text{l}$  of 1X Sperm Media solution with zinc (154.2  $\mu\text{l}$   $\text{H}_2\text{O}$ , 40  $\mu\text{l}$  5X Sperm Media, 4  $\mu\text{l}$   $\text{ZnCl}_2$  (.05 M), and 1.8  $\mu\text{l}$  20% dextrose). The slides were then incubated in a humid chamber for 15 minutes. After that, 1  $\mu\text{l}$  of worm homogenate (squashed) and 5  $\mu\text{l}$  Shelton's Medium were added to the solution. After dissecting males in both types of worm homogenate, the worm homogenate prepared by squashing proved superior to its counterpart

prepared by grinding, most likely due to its higher osmolality. Thus, it was used in this final phase of trials. Hermaphrodites, of a singular strain, were then added to the solution and dissected. Cover slips were then placed on the slides. They were then analyzed using a compound microscope via DIC microscopy and TR fluorescent filters.

### *C.) Results*

The first series of IVF experiments resulted in an extremely hypotonic environment for the oocytes. Oocytes would either lyse completely or expel their contents into the solution. In addition, spermatids dissected from CB4885 males did not undergo any activation. AV285 males did not release very many sperm after dissection. The dissected sperm tended to clump and remain stuck to the carcass preventing any significant sperm-oocyte interactions. Although numerous instances of contact between oocytes and sperm occurred, no fertilization happened.

The second series of IVF experiments tested two solutions. Sperm activation did not occur in any of the solutions. The status of oocytes varied greatly. Solutions ranged from hypotonic to hypertonic as different ratios of the two solutions were utilized. After evaluating the presence of PVP and BSA on wild-type (N2) embryonic development, PVP and BSA were abandoned in future trials.

The next series, which combined sperm media and egg buffer into one solution resulted in deformed spermatids and oocytes. Sperm exhibited spiky, triangular, and spherical appearances. Only CB4855 males were used because they produced a significantly greater quantity of sperm than other male strains that was also easier to distribute in solution. Similar to previous experiments, oocytes looked vacuolated and the solution appeared hypotonic.

The next series, of experiments incorporated dried synthetic porcine mucin. Initial attempts using the mucin failed to yield any observable results because the mucin obscured oocytes and made it nearly impossible to distinguish sperm when viewed by DIC microscopy. Wild-type embryos were then evaluated in egg buffer on mucin slides. All embryos either failed to hatch or appeared to die, perhaps due to various preservatives in the mucin. After this revelation, mucin was no longer used in future experiments.

The fifth phase of IVF experiments exhibited promising results. Activated sperm was seen moving in the solution and sperm-oocyte interactions were observed. Although the activated sperm interacted with the surface of oocytes, no fertilization occurred. Additionally, a larger proportion of sperm were found to be activated using the 4  $\mu$ l of .05 M ZnCl<sub>2</sub> solutions. Although most oocytes appeared healthy, some were shrunken and appeared to be in a hypotonic condition.

The final phase of IVF experiments offered the most promising results. Activated sperm was seen in the solution and oocytes generally mirrored *in vivo* conditions (Figure 15). Ultimately, no actively dividing embryos were observed. However, there was indirect evidence of fertilization. For example, oocytes were initially photographed as circular or irregularly shaped. Then in several cases, morphological changes occurred resulting an oval shape of the specimen (Figures 16, 17). This change may indicate the formation of embryos, but no further development was observed. In addition, the pronucleus of one oocyte was documented and then disappeared in future photographs, despite adjacent oocytes maintaining their pronucleus (Figure 18).

#### D.) Discussion

IVF has the potential to provide new information and insights into sperm-oocyte interactions. IVF would enable a more comprehensive understanding of the spatial, temporal, and environmental aspects of fertilization [13]. Furthermore, due to the genetic homology between the *C. elegans* and humans, *C. elegans* IVF may help us gain a better understanding of mammalian fertilization and various pathologies [6, 41].

Over the course of my research, my protocol evolved to try and best mimic *in vivo* conditions. This has culminated in a two phase experimental procedure involving Shelton's Media, worm homogenate (squashed), and 1X Sperm Media containing  $ZnCl_2$ . The osmolality of this final solution is approximately 285 mMol/kg.

An IVF solution is inherently difficult to create because one must construct an artificial media without knowing the *in vivo* conditions that need to be mimicked. As *C. elegans* is roughly 1 mm long, determining *in vivo* conditions in the uterus is impossible. pH, temperature, and osmolality are among a few of the variables to consider in synthesizing any IVF solution. This two phase protocol operates under the assumption that spermatozoa are more resistant to changes in osmotic pressure than are spermatids. Thus, by activating the spermatids initially, they will remain fertilization competent when an embryo-compatible solution is introduced. Moreover, worm homogenate was introduced to increase the motility of spermatozoa in solution (unpublished results from Dr. Long Miao). Shelton's Medium was introduced only after fertilization failed to occur with egg buffer in the second phase.

The experimental results strongly suggest the possibility of fertilization *in vitro*, but do not provide direct, consistent evidence of IVF. The observed morphological changes,

disappearing pronucleus, and formation of apparent embryos arrested in development provide tantalizing support for IVF. However, with the lack of concrete evidence no conclusions can be drawn about the fertilization competence of nonEmo oocytes by *in vitro* activated sperm.

## IV: Creating Mermaid-2 Expression in *C. elegans*

### A.) Introduction

#### a. Fertilization in Various Species

In general, fertilization occurs when two haploid cells fuse together [14], and this fusion initiates an increase in the free calcium intracellular concentration. Embryonic activation then occurs, and the quiescent oocyte becomes biosynthetically active and initiates embryonic development [18, 41]. Understanding the mechanisms behind fertilization in various model organisms will help to better understand human fertilization. It also carries potential for the treatment of human pathologies, the most important of which is infertility [41].

Sea urchins are marine invertebrate animals that have emerged as invaluable model organisms to study fertilization. In nature, the egg secretes a protein, called resact in the case of *Arbacia punctulata*, which chemically attracts sperm to it [42]. Through a series of reactions, fertilization subsequently occurs. To prevent multiple sperm from penetrating the oocyte, the sea urchin has developed highly efficient blocks to polyspermy [16]. The fast block preventing polyspermy utilizes a rapid depolarization of the embryo's membrane potential [43]. In fact, applying current to maintain a positive voltage prevents any fertilization. Conversely, polarizing the embryo, either chemically or physically, in the presence of sperm results in polyspermy. Similar findings were found in starfish, echiuroid worms, and frogs [44]. In addition, sea urchins exhibit a second slow block to polyspermy mediated by the cortical granule reaction, which is thought to be triggered by a calcium influx [45]. Cortical granules fuse with the vitelline membrane, exocytose their contents, and an impenetrable fertilization coat is created [46].

In mice, the only currently known protein regulating sperm-oocyte interaction is IZUMO1, which plays a critical role in the fusion of sperm to the oocyte after the acrosome reaction [47]. After the sperm has fused with the oocyte, a calcium influx triggers embryonic activation. This results in a variety of downstream effects, but of particular interest are the cortical granule exocytosis and blocks to polyspermy [18]. The fast block to polyspermy in mammals is not well understood, and might not exist. However, it is known that increased intracellular free  $\text{Ca}^{++}$  is essential. Furthermore, multiple oscillations of  $\text{Ca}^{++}$  concentrations must occur for normal embryonic activation and subsequent development. Mice embryos exposed to only one  $\text{Ca}^{++}$  shift will only produce partial blocks to polyspermy [43]. It is known that various mammalian membrane blocks do not lead to a membrane depolarization as seen in the sea urchin [48]. Moreover, mice and many mammals also exhibit a slow block to polyspermy due to cortical granule exocytosis. This occurs when proteases, glycosidases, and cross-linking enzymes are released, that alter the zona pellucida to make it impermeable to sperm [18].

Similar to sea urchins, *C. elegans* oocytes secrete a chemical, polyunsaturated fatty acids, to attract sperm to the spermatheca. This is produced to guide male sperm ejaculated into the uterus to the spermatheca. It also is used to direct sperm back to the spermatheca after sperm were pushed into the uterus during ovulation [41]. Fertilization also results in an intracellular  $\text{Ca}^{++}$  increase, which is thought to trigger embryonic activation and embryogenesis in a manner that is not fully understood [18]. In contrast to other species, *C. elegans* cortical granule exocytosis does not aid in a membrane block but is thought to play a fundamental role in the formation of the chitin shell. However, *C. elegans* must possess a mechanistic block to

polyspermy, although its nature is currently unknown [18]. Recently, two genes, *egg-4* and *egg-5*, have been found to play essential roles in the formation of the chitinous embryo shell and the polyspermy block [49].

#### *b. Fertilization mutants in C. elegans*

In general, there are two classes of fertilization related mutants in *C. elegans*: *spe* (fertilization defective) and *egg* (egg defective) class mutants. *spe* class mutants exhibit aberrant spermatocytes, spermatids, spermatogenesis, spermiogenesis, and/or fertilization [18]. *spe-9* class (*fer-14*, *spe-9*, *spe-13*, *spe-36*, *spe-38*, *spe-41/trp-3*, *spe-42*, and *spe-45*) mutants are of a particular interest because they produce seemingly normal spermatozoa that are infertile yet can still outcompete hermaphroditic sperm [7]. Similar to IVF and its importance in *C. elegans* research, the Mermaid-2 voltage sensor could provide new insights and information about sperm-oocyte interactions, fertilization, and the ion shifts related to them.

#### *c. Mermaid-2 Voltage Sensor*

The Mermaid-2 voltage sensor is derived from a voltage-sensing phosphatase (Ci-VSP) in *Ciona intestinalis* [50]. Of specific interest is the voltage-sensor domain (VSD) that is composed of four transmembrane domains that undergo conformational changes in response to voltage shifts [51, 52]. Mermaid-2 is tagged with two variants of a green fluorescent protein isolated from sarcophyton coral: cyan fluorescent protein (CFP) and yellow fluorescent protein (YFP; Figure 19) [50]. When depolarization occurs, there is a conformational change in the protein that results in a CFP moving very close to a YFP allowing a yellow light emission, via fluorescence resonance energy transfer (FRET) [52]. In this process, energy is transferred from

a donor fluorophore (CFP) to a receptor fluorophore (YFP) through dipole-dipole coupling (Figure 20) [53]. FRET is observed within a molecular proximity of 10-100 Å, but is optimal if the donor-receptor pair are within the Förster radius (usually 3-6 nm) [54-57].

#### *d. Previous work with the Mermaid-2 Voltage Sensor*

The Mermaid-2 voltage sensor has previously been used in primarily two different model organisms: mice and zebrafish [52, 58]. In 2013, Mermaid-2 was utilized to investigate neurological electrical activity in mice. This voltage probe successfully detected electrical activity at and below an action potential threshold. In addition, Mermaid-2 was used to detect cortical electrical responses *in vivo* to sound stimuli [52]. The Mermaid voltage sensor was used in zebrafish to track the electrical depolarizations that occurred when cardiac muscle undergoes cycles of contraction and relaxation [58].

### *B.) Materials and Methods*

#### *i. Mermaid-2 Plasmid Synthesis*

##### *a. DNA Cloning and Amplification*

The first steps in synthesizing the *Mermaid-2* plasmid involved procuring and amplifying specific DNA constructs: the promoter (*glh-2*), pEJG30 (*Mermaid-2*), pCFJ151 (*MosSCI*), and *fbf-2* (3'-UTR).

*glh-2* and *fbf-2* were both amplified using the polymerase chain reaction (PCR) [59]. Forward and reverse primers were ordered from Integrated DNA Technologies (Figure 21). PCR was performed with Platinum HotStart Master Mix (Invitrogen) as described in their protocol. A PTC-100 Peltier Thermal Cycler was used to regulate the denaturing, annealing, and extension stages of PCR.

pCFJ151 (MosSCI) was ordered from AddGene (Plasmid #19330). A construct of Mermaid-2 that was codon-optimized and contained *C. elegans* introns was synthesized by Invitrogen GeneArt Gene Synthesis. Both constructs were transferred into high efficiency NEB DH5- $\alpha$  competent *E. coli* cells, and grown overnight via a protocol from New England Biolabs. Each liquid culture was then mini-prepped to isolate plasmid DNA using the Zypzyk Plasmid Miniprep Kit, as per the supplied instructions. pEJG30 was restriction digested with the *SrfI* restriction enzyme to cleave the plasmid into 2.2 kb and 2.8 kb segments. Similarly, pCFJ151 was restriction digested with *SfiI* restriction enzyme. *SfiI* is a blunt cutter that created a single cleavage in the plasmid. Restriction digests were then analyzed using gel purified (Zymo).

#### *b. Gibson Cloning*

The DNA fragments were then combined with 30 bp overlapping regions using Gibson Cloning, according to the NEB protocol [60]. Figure 22 illustrates the completed plasmid, pHP1, which was prepped and sequenced (GENEWIZ).

#### *ii. Mos1-mediated Single Copy Insertion (MosSCI)*

Once pHP1 was sequence-verified, Dr. John Ahn in the Kelly Lab at Emory University performed MosSCI insertion. MosSCI utilizes the Mos1 transposon to create a double strand break in DNA on at a defined site on chromosome 2. The break can then be repaired via insertion of an extra chromosomal template. By microinjecting pHP1 into the *C. elegans*, a transgenic line can form because pHP1 can serve as that extra chromosomal template. Additionally, even if chromosomal integration does not occur, an extra chromosomal array may result. pHP1 was co-injected with positive and negative markers. EG6699 *MosSCI on II, unc-119 (III)* was used as the recipient *C. elegans* line. *unc-119* expression results in a nearly

paralyzed, semi-fertile worm. If recombination occurs via MosSCI, a non *unc-119* phenotype would be observed. Additionally, three different plasmids (pCFJ90, pGH8, and pCFJ104) coding for red fluorescence were co-injected. This negative control differentiates integrated transgenes and extra chromosomal arrays as the red fluorescence is only expressed in extra chromosomal arrays [61, 62].

### *iii. Microscopy and Imaging*

Laura Fox-Goharioon, a member of Emory University's Integrated Cellular and Image Core, assisted in using a Leica TCS SP8 Confocal Microscope to examine and image transgenic Mermaid-2 worms suspended in a 0.6 mM Levamisol solution. CFP and YFP emissions were 348-383 nm and 527-547 nm, respectively.

### *C.) Results*

After MosSCI, several recombinant lines formed. Two lines displayed integrated chromosomal recombination, and one was an extra chromosomal array. Integrated chromosomal recombination was only observed after the second generation, mirroring expected MosSCI results [62]. However, no Mermaid-2 linked fluorescence was detected. Upon review of the pHP1 sequence, an unintended upstream start codon was found at the linkage of the Mermaid-2 and *glh-2* sequences. To remedy this problem, a new plasmid, pEJG37 (Figure 22), was synthesized using an identical protocol, except this time, Mermaid-2 was restriction enzyme digested with *StuI* to remove the upstream TG portion of the start codon. In addition, different primers were also used to replicate the DNA fragments (Figure 23). Lastly, *mex-5* replaced *fbf-2* as the 3'-UTR region because it allows better expression in oocytes [63] (Figure 24). *mex-5* (pBAB96) was a gift from Dr. Elizabeth Bowman from the Kelly

Lab at Emory University. Figure 25 provides the corrected sequence containing *glh-2*, Mermaid-2, and *mex-5*.

After MosSCI injection was performed by Dr. Ahn, two independent integrated lines emerged. These lines were analyzed with the Leica TCS SP8 Confocal Microscope and the presence of both CFP and YFP was confirmed in the germline (Figure 26). The yellow signal, suggesting FRET, was observed in the proximal gonad arm, spermatheca, and uterus. No yellow flashes were observed that would indicate sudden calcium fluctuations. It is still unknown what this reveals about the calcium gradients present during *C. elegans* fertilization.

#### *D.) Discussion*

MosSCI was chosen as the primary transgenic technique because it enabled integration in to chromosome II in *C. elegans*. Transgenic integration results in more normalized expression than what occurs from extrachromosomal arrays [62]. Moreover, extrachromosomal arrays have inconsistent transmittance and are far more sensitive to genetic silencing, especially in *C. elegans* germ cells [64, 65].

The Mermaid-2 voltage sensor has a high potential as an investigative tool for *C. elegans*. The successful creation of transgenic lines exhibiting FRET between CFP and YFP signals may enable the visualization and study of calcium concentration changes related to sperm-oocyte interactions. It could also provide insight into polyspermy blocks in *C. elegans*.

Moreover, the Mermaid-2 voltage sensor could offer a mechanism by which to further differentiate and understand various *spe*, *fer*, and *egg* mutants. The *spe-9* class mutants are of interest because they produce motile spermatozoa that contact oocytes but are unable to successfully fertilize them. Male sperm from *spe-9*, *spe-13*, *spe-41/trp-3*, or *spe-42* mutants

renders the hermaphrodite infertile [7]. This is because these male-derived sperm, even if they are fertilization-defective, can invariably outcompete hermaphroditic sperm [11]. *spe-41*, *spe-9*, *spe-42*, *spe-45*, *fer-14*, and *spe-38* mutants all have defects in plasma membrane proteins found in spermatozoa, suggesting a faulty role in sperm-oocyte surface interactions [7]. Several of these genes are orthologous to mammalian genes and could provide insight into human fertilization [6].

## Chapter V: Future Directions

The presented data and experimental protocols have yielded promising results, however much future work must be done regarding IUF, IVF, and the Mermaid-2 voltage sensor.

The IUF experiments thus far are highly suggestive that nonEmo oocytes from *pezo-1* mutants remain competent for fertilization *in utero*, spermatozoa do not require a physiological change found only in the spermatheca, and IVF may be possible. Future work should employ a male line in which GFP is expressed in the sperm. This would allow for simple, direct observation of sperm *in vivo* after mating. In addition, it could provide unequivocal evidence for the exact location of fertilization both *in vivo* and on the oocyte. The goal of future work is documenting the actual fertilization event and embryonic development *in utero*. This would decisively validate claims of nonEmo oocyte competence and the lack of a 'capacitation' event at the spermatheca.

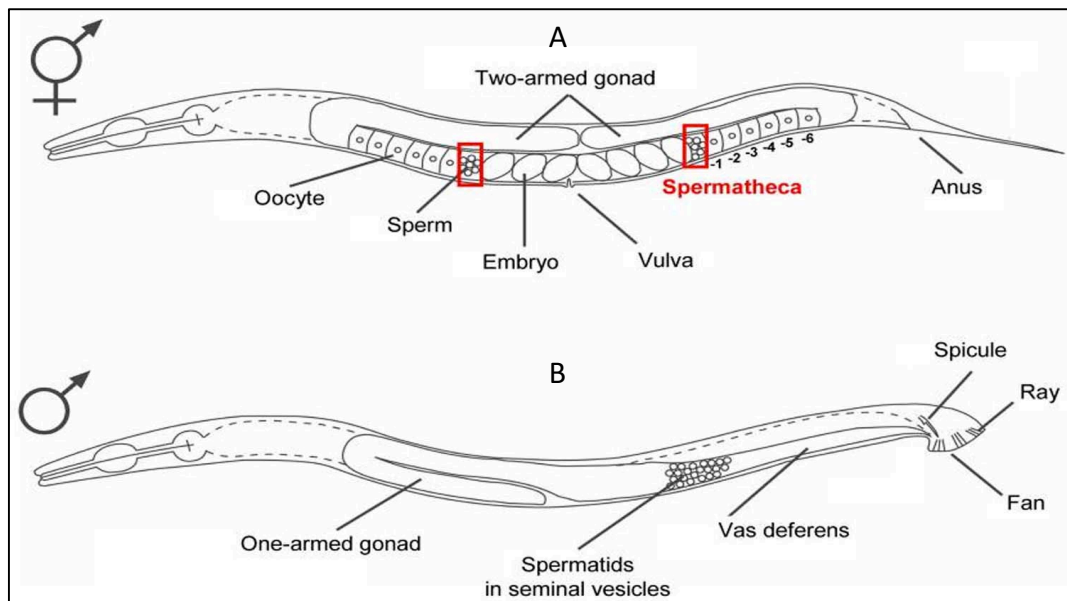
IVF in *C. elegans* carries enormous scientific potential. It would allow unobstructed observation of spatial, temporal, and environmental influence on fertilization [13]. Furthermore, due to the genetic homology between the *C. elegans* and humans, *C. elegans* IVF may help us gain a better understanding of mammalian fertilization and various pathologies [6, 41]. Thus, IVF research must be continued.

First, a better IVF solution must be developed. The current IVF protocol utilizing 1X Sperm Media with ZnCl<sub>2</sub>, Shelton's Media, and worm homogenate (squashed) yields a wide variety of oocyte and sperm cytology. Future media should maximize the number and motility of activated sperm. It should also be compatible with oocytes, especially regarding osmolality. It is currently unknown what components should be added or subtracted to this solution to

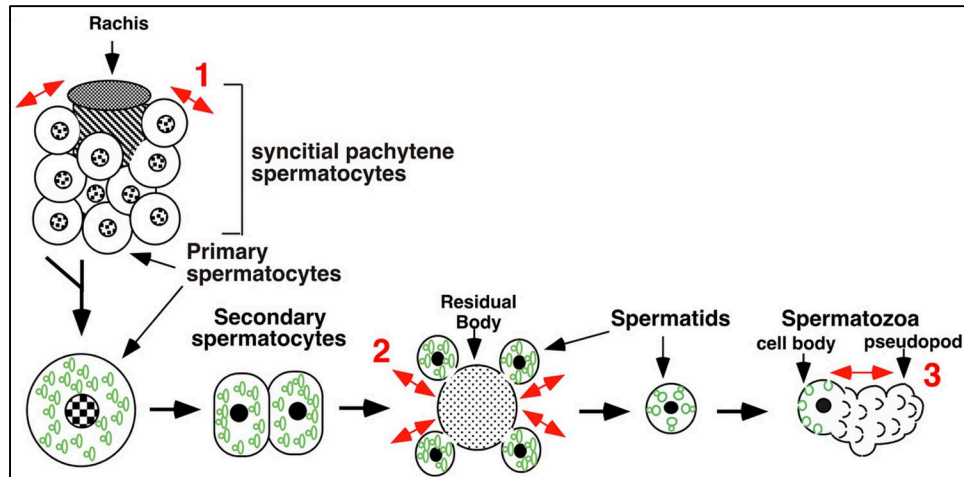
allow for successful fertilization *in vitro*, but future studies may integrate IVF media from rabbits, humans, or other species in which IVF has successfully been documented. If indisputable IUF occurs, the male and hermaphroditic mutant lines in that experiment should be utilized for IVF.

The successful creation and integration of the Mermaid-2 vector in *C. elegans* offers a novel technique to study fertilization. As previously stated, this optogenetic tool may enable the visualization and study of  $\text{Ca}^{++}$  or other ionic concentration changes related to sperm-oocyte interactions. It could also provide insight into polyspermy blocks in *C. elegans*. Future work must be done on *spe-9* class mutants not only for their classification, but for a broader understanding of biochemical processes during fertilization in *C. elegans*. This would largely be done through FRET microscopy.

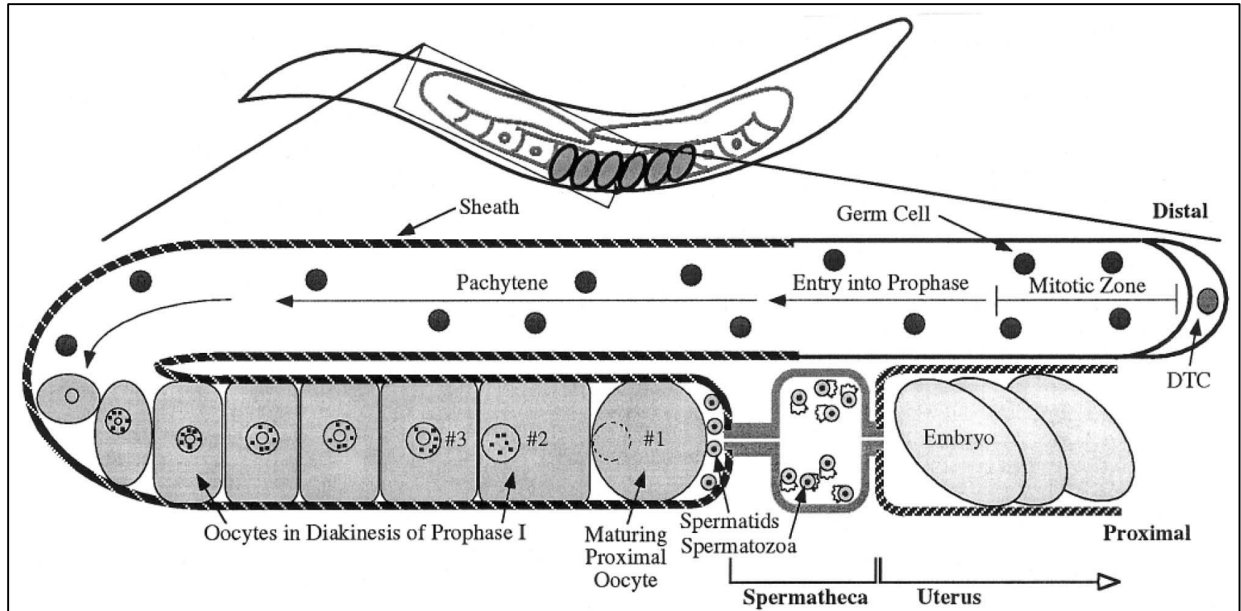
## Figures and Tables



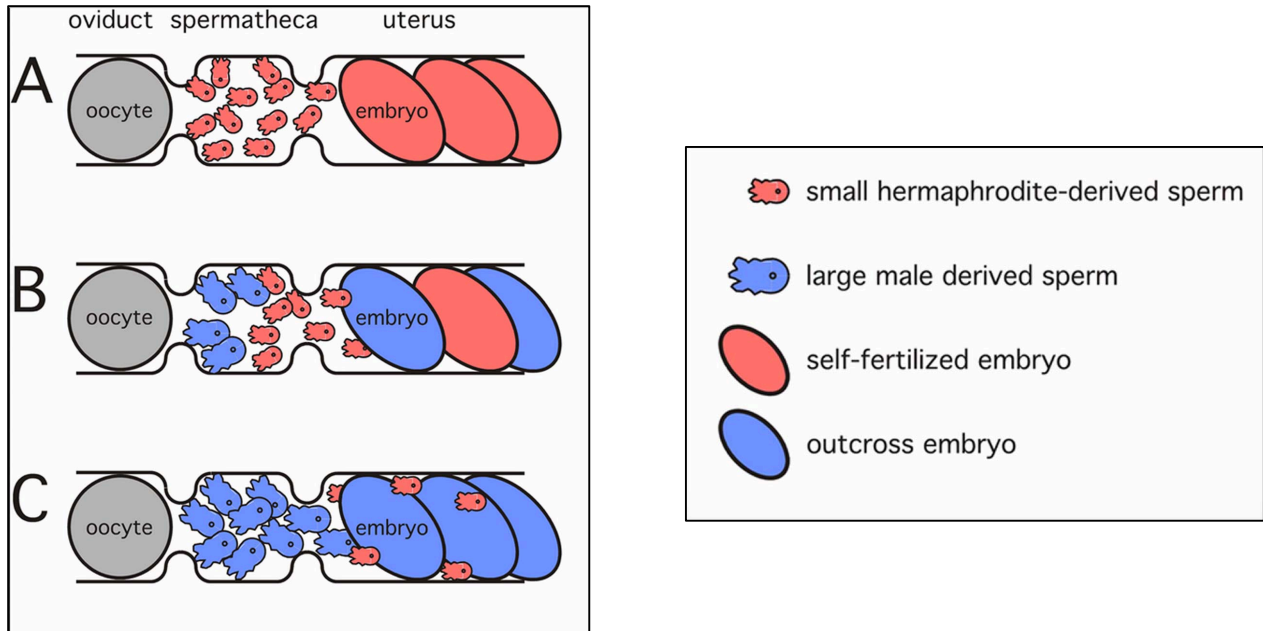
**Figure 1:** The reproductive anatomy of an *C. elegans*. Figure 1A shows the hermaphrodite with a bisymmetric two-armed gonad. As germ cells develop into oocytes, they travel from the distal gonad arm to the proximal gonad arm. Eventually they encounter the spermatheca, outlined in red rectangles, where fertilization occurs. Embryos then align *in utero* until they are expelled through the vulva. Figure 1B shows the reproductive anatomy of the adult male *C. elegans*. It has a one-armed gonad that stores spermatids in the seminal vesicle until they are ejaculated during mating. This image is modified from Nishimura & L'Hernault, 2010.



**Figure 2:** Overview of spermatogenesis. Red numbers highlight major asymmetric events in this process. 1, primary spermatocytes bud off from the rachis. Then these primary spermatocytes undergo the first meiotic division resulting in two secondary spermatocytes. In this diagram they are shown attached, but in reality, they can be separated or attached. 2, meiotic division II occurs resulting in spermatids. Spermatids have specifically sequestered specialized secretory lysosome named fibrous body-membranous organelles (FB-MO's) shown in green. 3, spermiogenesis occurs as MO's fuse with the plasma membrane and a pseudopod forms. This image is modified from L'Hernault, 2006.



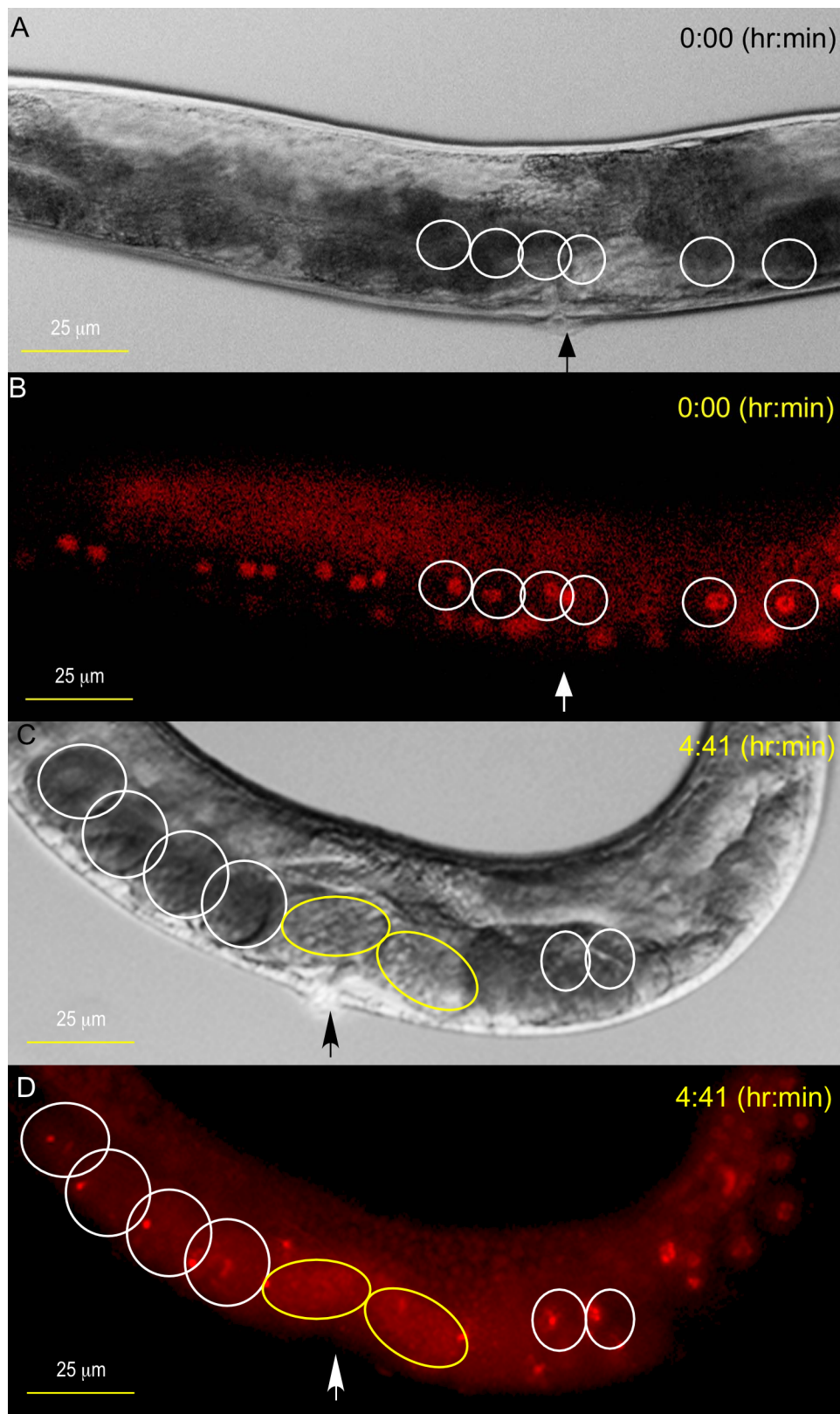
**Figure 3:** An overview of oogenesis and self-fertilization in *C. elegans* hermaphrodites. One half of the two bisymmetric gonad arm is shown at the bottom of the figure. Germ cells begin development in the distal gonad arm and mature as they travel proximally to the spermatheca. As oocytes approach the spermatheca, they are arrested in diakinesis of prophase I of meiosis I. As they encounter the spermatheca, they will push spermatids forward, activating spermiogenesis and thus forming fertilization competent spermatozoa. After fertilization, the embryo will complete meiosis I and II *in utero*. This image is modified from McCarter, Bartlett, Dang, & Schedl, 1999.



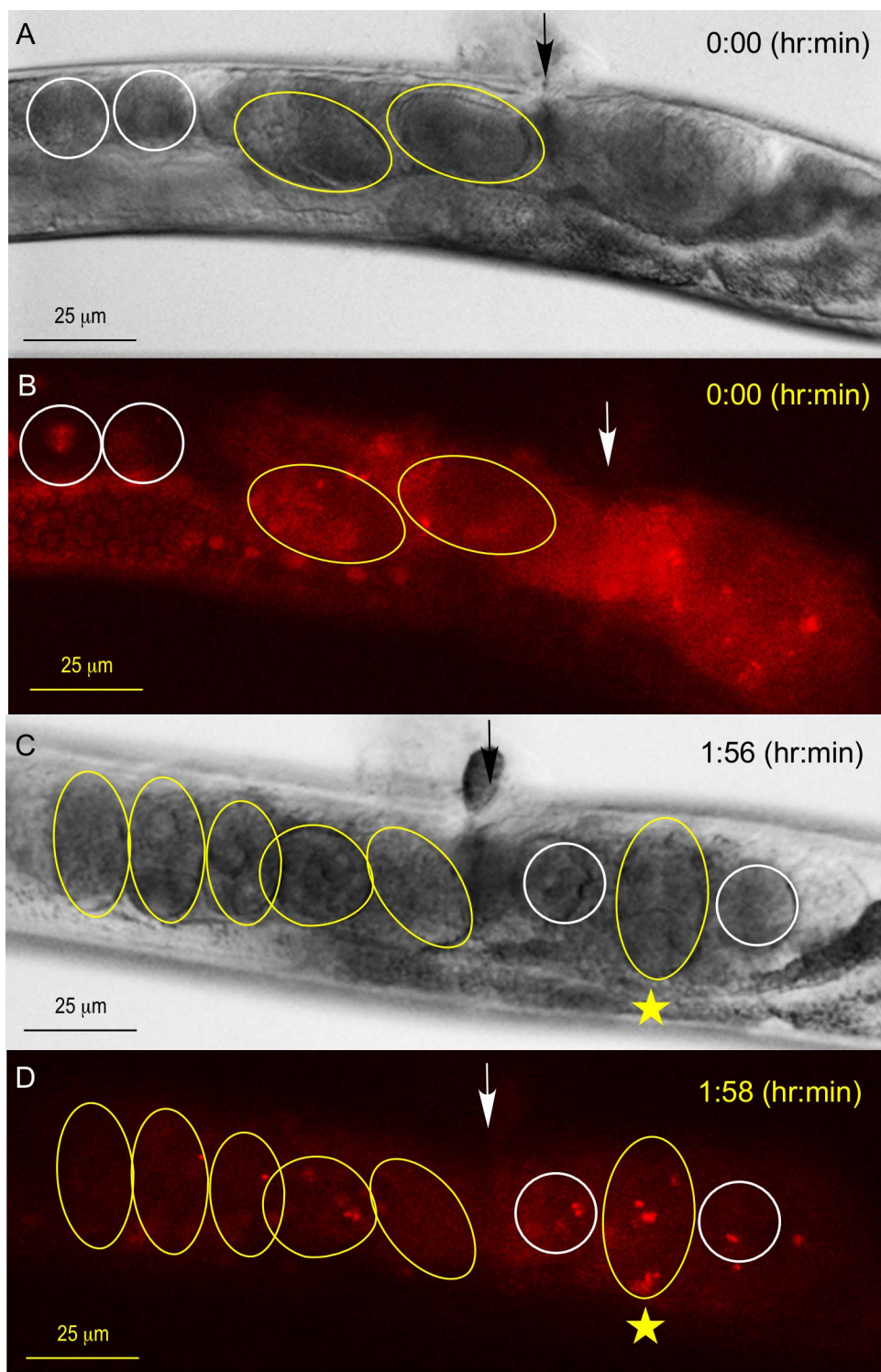
**Figure 4:** Self-fertilization and sperm competition in *C. elegans*. As oocytes pass through the spermatheca, they are fertilized by hermaphrodite-derived sperm. 4B and 4C illustrate the suppression of self-fertilization if male sperm are present in the spermatheca. This image is modified from L'Hernault, 2006.

| SL Designation | Genotype  | Relevant Phenotypic Features  | Purpose  |
|----------------|---|---|--|
| SL1607         | <i>fer-1(b232ts) I; pezo-1(gk894716) IV</i>   | <ul style="list-style-type: none"> <li>• nonEmo (<i>pezo-1</i>)</li> <li>• infertile at 25°C (<i>fer-1</i>)</li> </ul>  | <ul style="list-style-type: none"> <li>• Hermaphrodite in IUF experiments (Phase 4)</li> <li>• Oocyte donor in IVF experiments (All phases)</li> </ul> |
| SL1651         | <i>fer-1(b232ts) I; dpy-20(e1282) itIs37 [(pAA64) pie-1p::mCherry::his-58 + unc-119(+)] pezo-1(ebDf1) IV; itIs38[pAA1; pie-1::GFP::PH(PLC1delta1) + unc-119(+)]</i> | <ul style="list-style-type: none"> <li>• Red fluorescent nuclei (<i>itIs37</i>)</li> <li>• Green fluorescent cytoplasm (<i>itIs38</i>)</li> <li>• nonEmo (<i>pezo-1</i>)</li> <li>• infertile at 25°C (<i>fer-1</i>)</li> </ul> | <ul style="list-style-type: none"> <li>• Hermaphrodite in IUF experiments (Phase 1)</li> </ul>   |
| SL1655         | <i>fer-1(b232ts) I; dpy-20(e1282) itIs37 [(pAA64) pie-1p::mCherry::his-58 + unc-119(+)] pezo-1(ebDf1) IV</i>  | <ul style="list-style-type: none"> <li>• Red fluorescent nuclei (<i>itIs37</i>)</li> <li>• nonEmo (<i>pezo-1</i>)</li> <li>• infertile at 25°C (<i>fer-1</i>)</li> </ul>  | <ul style="list-style-type: none"> <li>• Hermaphrodite in IUF experiments (Phases 1,2)</li> </ul>  |
| SL1698         | <i>spe-9(hc88ts) I; dpy-20(e1282) ItIs37 [(pAA64) pie-1p::mCherry::his-58 + unc-119(+)] pezo-1(ebDf1) IV</i>  | <ul style="list-style-type: none"> <li>• Red fluorescent nuclei (<i>itIs37</i>)</li> <li>• nonEmo (<i>pezo-1</i>)</li> <li>• infertile at 25°C (<i>spe-9</i>)</li> </ul>  | <ul style="list-style-type: none"> <li>• Hermaphrodite in IUF experiments (Phase 3)</li> <li>• Oocyte donor in IVF experiments (Phase 6)</li> </ul>    |
| CB4855         | <i>C. elegans wild isolate plg-1(e2001) III</i>   | <ul style="list-style-type: none"> <li>• Forms copulatory plugs (<i>plg-1</i>)</li> <li>• 2) Male line</li> </ul>   | <ul style="list-style-type: none"> <li>• Male in IUF experiments (Phase 2)</li> <li>• 2) Sperm donor in IVF (Phases 1-5)</li> </ul>                    |
| SL1699         | <i>plg-1(e2001) III; hjSi20 [myo-2p::mCherry::unc-54 3'UTR] IV</i>  | <ul style="list-style-type: none"> <li>• Forms copulatory plugs (<i>plg-1</i>)</li> <li>• Male line</li> <li>• Red pharynx (<i>hjSi20</i>)</li> </ul>   | <ul style="list-style-type: none"> <li>• Male in IUF experiments (Phases 3,4)</li> <li>• Sperm donor in IVF (Phase 6)</li> </ul>                       |
| AV285          | <i>swm-1(me66); him-5(e1490) V</i>  | <ul style="list-style-type: none"> <li>• Inherently activated sperm (<i>swm-1</i>)</li> <li>• Male line (<i>him-5</i>)</li> </ul>   | <ul style="list-style-type: none"> <li>• Sperm donor in IVF experiments (Phases 1, 2)</li> </ul>   |
| SL1352         | <i>zuls178 [(his-72::HIS-72::GFP::his-72); unc-119(+)]; him-8(e1489) IV</i>   | <ul style="list-style-type: none"> <li>• Green fluorescent nuclei (<i>zuls178</i>)</li> <li>• Male line (<i>him-8</i>)</li> </ul>   | <ul style="list-style-type: none"> <li>• Male in IUF experiments (Phase 1)</li> </ul>  |

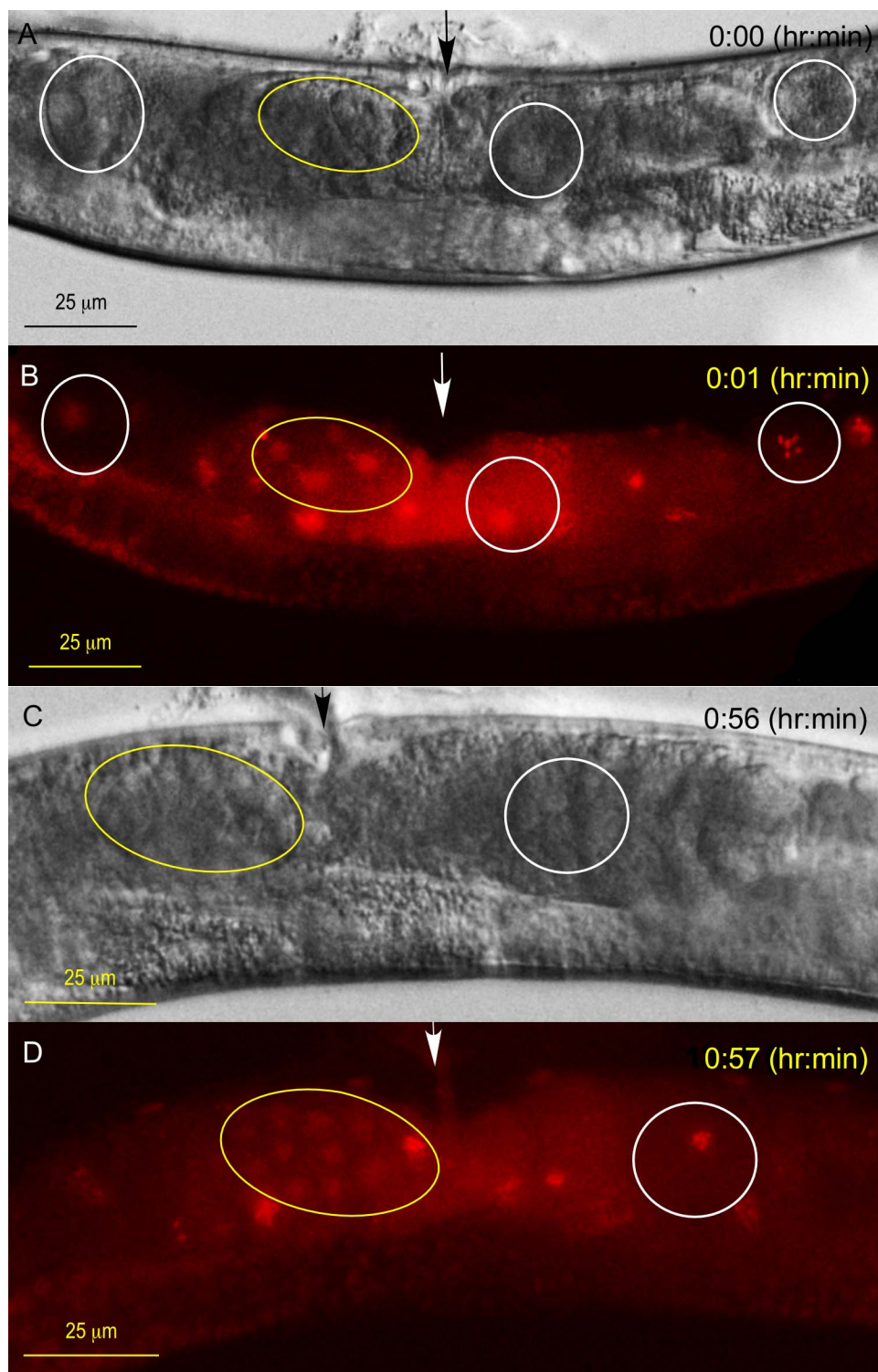
**Table 5:** Mutant strains used during *in utero* and *in vitro* experiments.



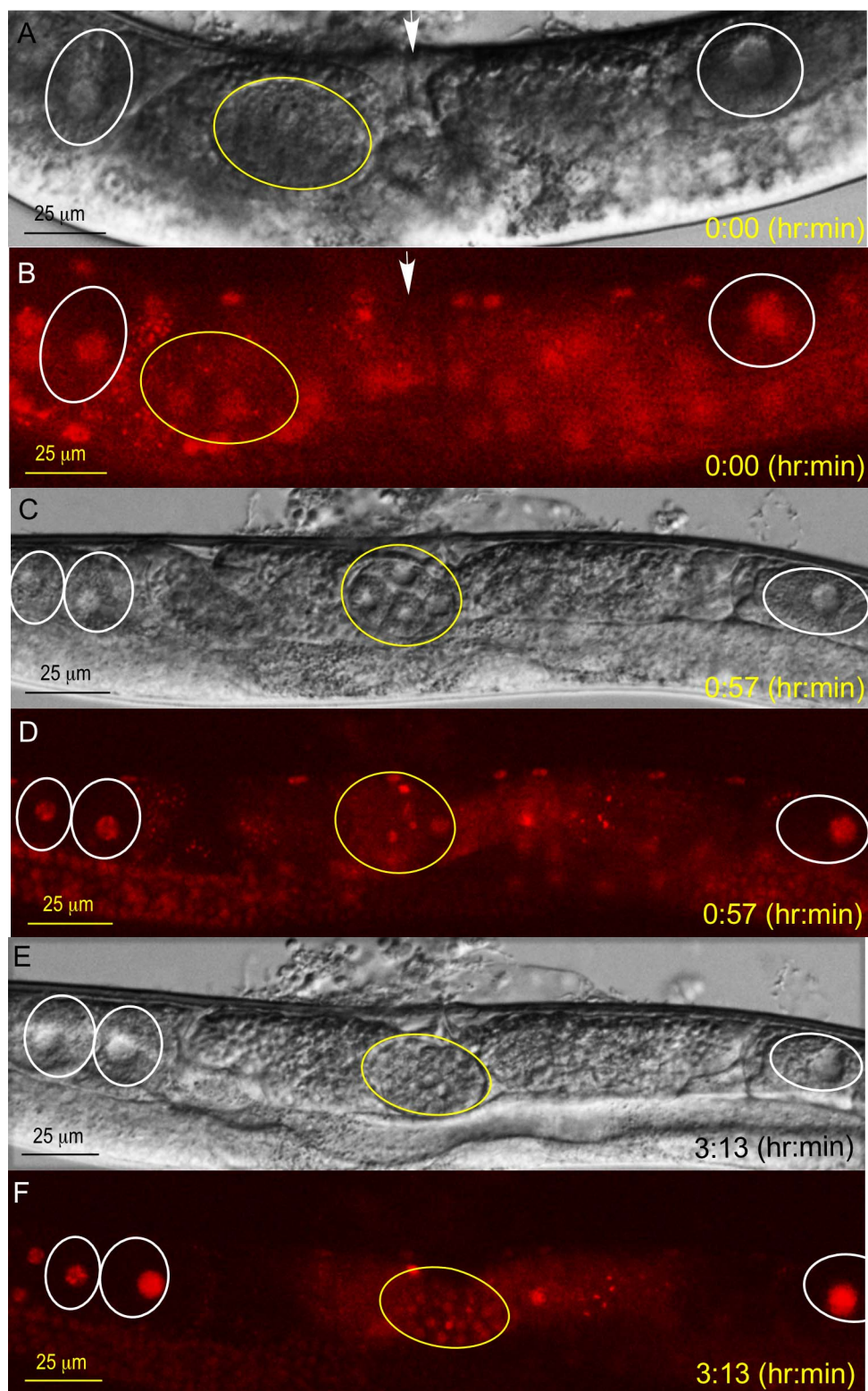
**Figure 6:** Phase 1 IUF trial using SL1352 male worms and SL1651 hermaphrodites. Black and white photographs were taken with DIC microscopy and the red fluorescence was captured with a Texas Red (TR) filter. Oocytes are circled in white, and embryos are circled in yellow. In each picture an arrow identifies the vulva. Overall, the chronological development of embryos that were likely to be fertilized *in utero* is shown. The initial photographs (A, B) show no embryos at the start of observation. In C and D, two embryos can be seen developing directly behind the vulva. Additionally, oocytes are seen lined up behind those embryos *in utero*.



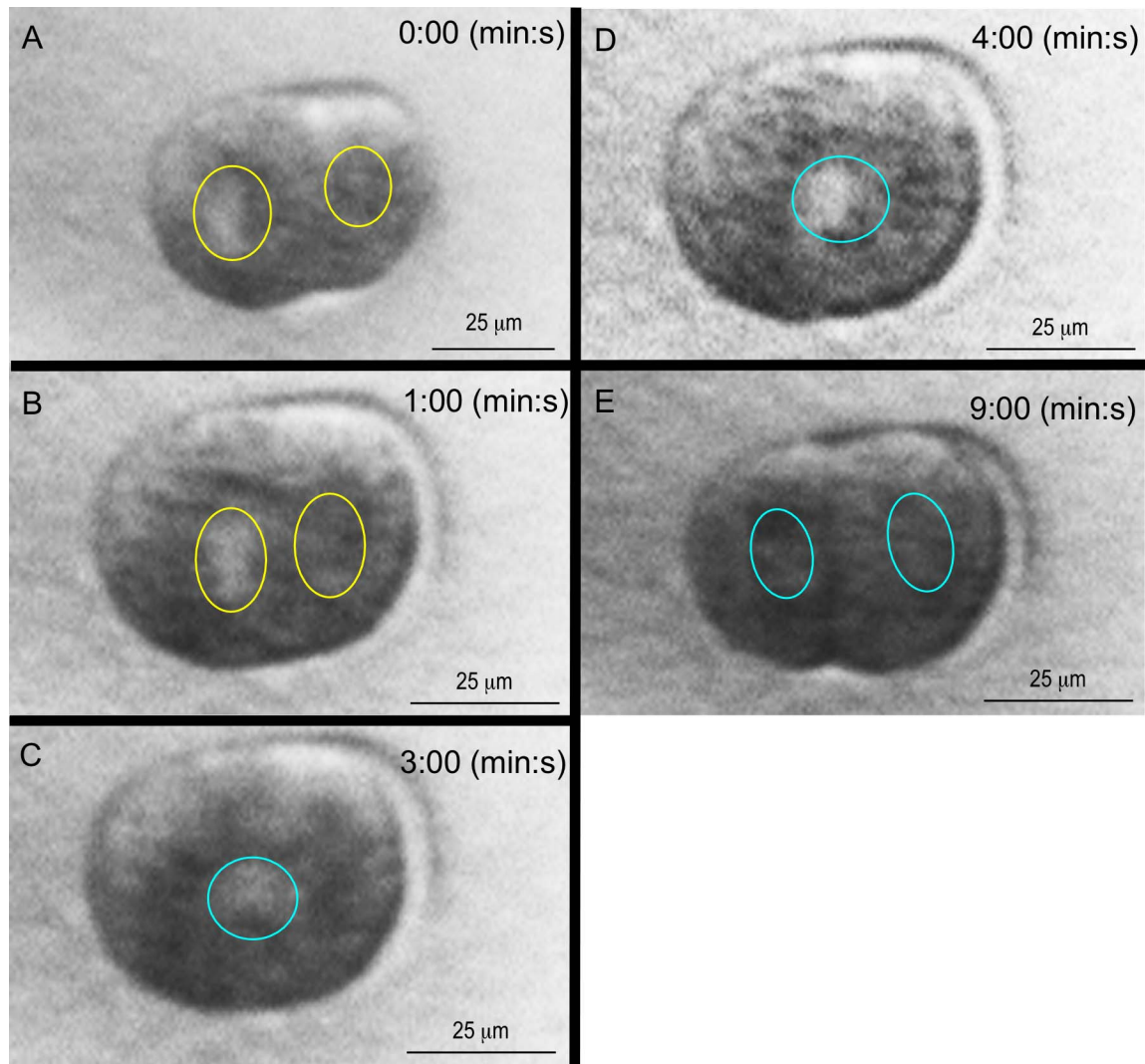
**Figure 7:** The results of an IUF phase 1 trial involving SL1352 *zuls178* male worms and SL1651 hermaphrodites. Black and white photographs were taken with DIC microscopy and the red fluorescence was captured with a TR filter. Oocytes are circled in white, and embryos are circled in yellow. In each picture an arrow identifies the vulva. C and D show the presence of an embryo in between two oocytes. The left gonad arm contains a uniform series of five embryos. However, the right gonad arm showcases an unexpected order of oocytes and embryos if fertilization were to occur in the spermatheca. This would suggest fertilization occurred outside of the spermatheca.



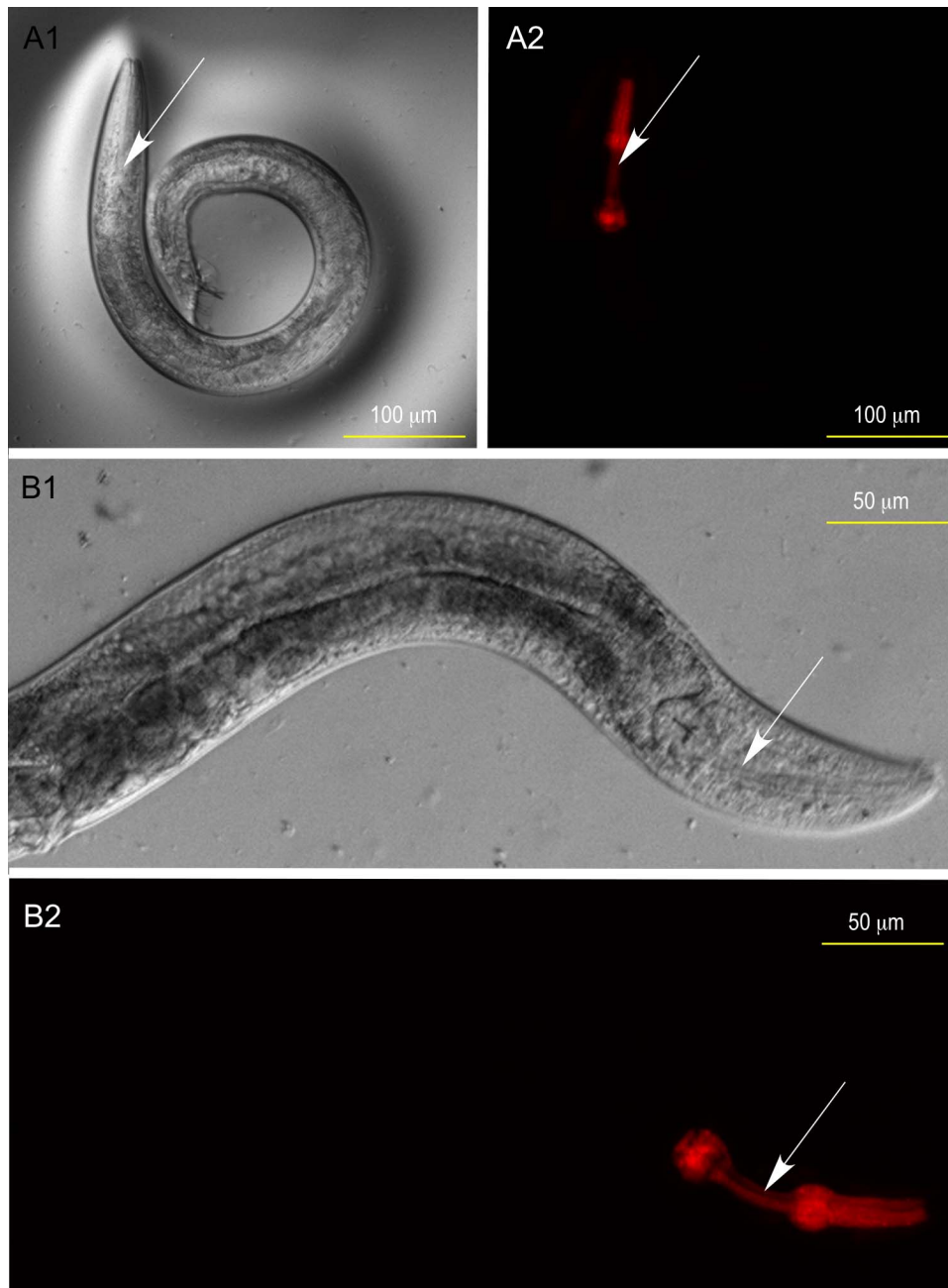
**Figure 8:** The results from an IUF Phase 2 trial utilizing CB4855 males and SL1655 hermaphrodites. Black and white photographs were taken with DIC microscopy and the red fluorescence was captured with a TR filter. Oocytes are circled in white, and embryos are circled in yellow. A and B were taken immediately after observing the presence of the copulatory plug on a hermaphrodite. In the first two photographs, a four-cell embryo can be seen directly behind the vulva. After one hour, this embryo had developed to the 30-cell stage (C, D). The embryo was likely not expelled from the uterus because the worm was paralyzed in a 0.2mM levamisol solution.



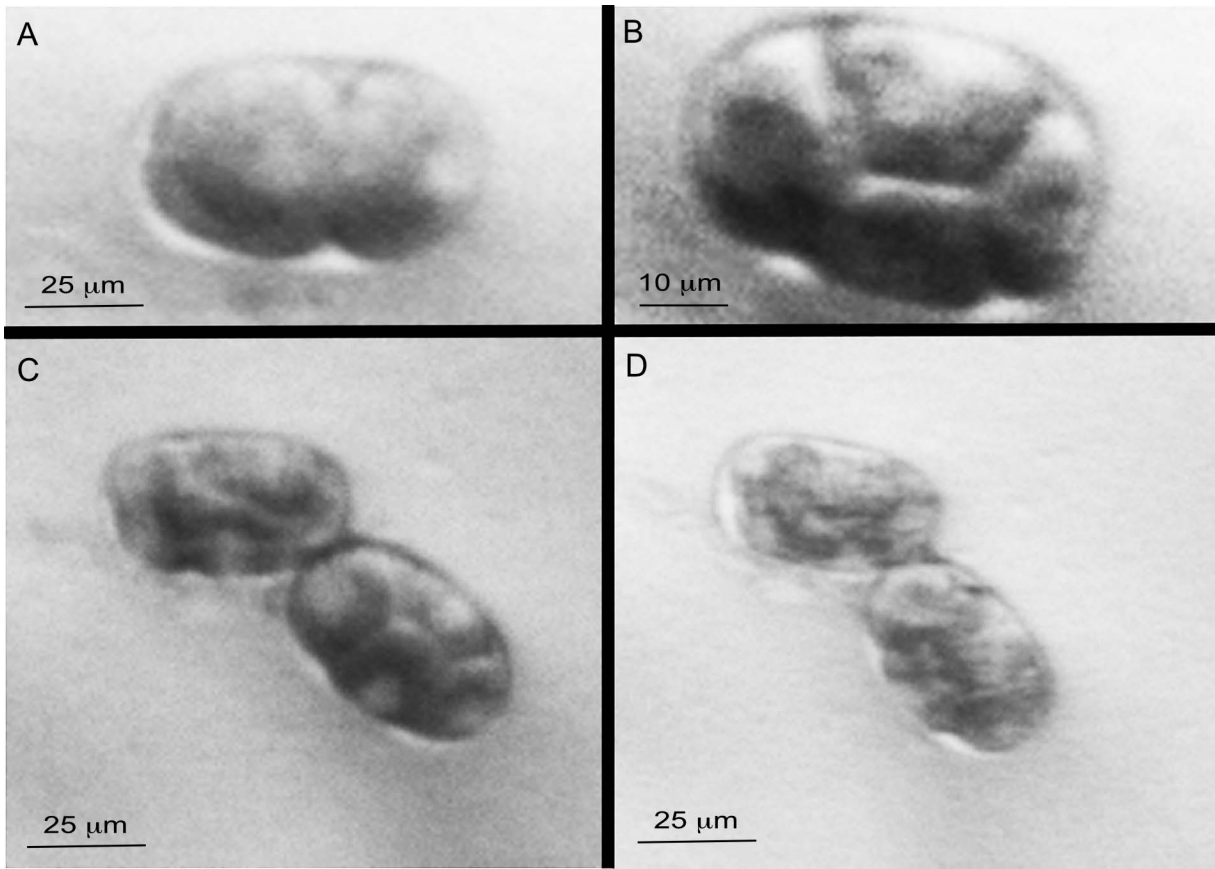
**Figure 9:** The results of the third phase of IUF trials. SL1699 males and SL1698 hermaphrodites were used in this trial. Black and white photographs were taken with DIC microscopy and the red fluorescence was captured with a TR filter. Oocytes are circled in white, and embryos are circled in yellow. In each picture an arrow identifies the vulva. This figure provides a chronological visual of the embryonic development *in utero*. A newly shelled zygote is initially seen and documented *in utero* (9A and 9B), and 57 minutes later, it is a four-celled embryo is observed directly behind the vulva (Figure 9C and 9D). This is highly suggestive of *in utero* fertilization since it would have taken an hour for the sperm to reach the spermatheca plus another 30 and 40 minutes to develop into a four-celled embryo after fertilization [22].



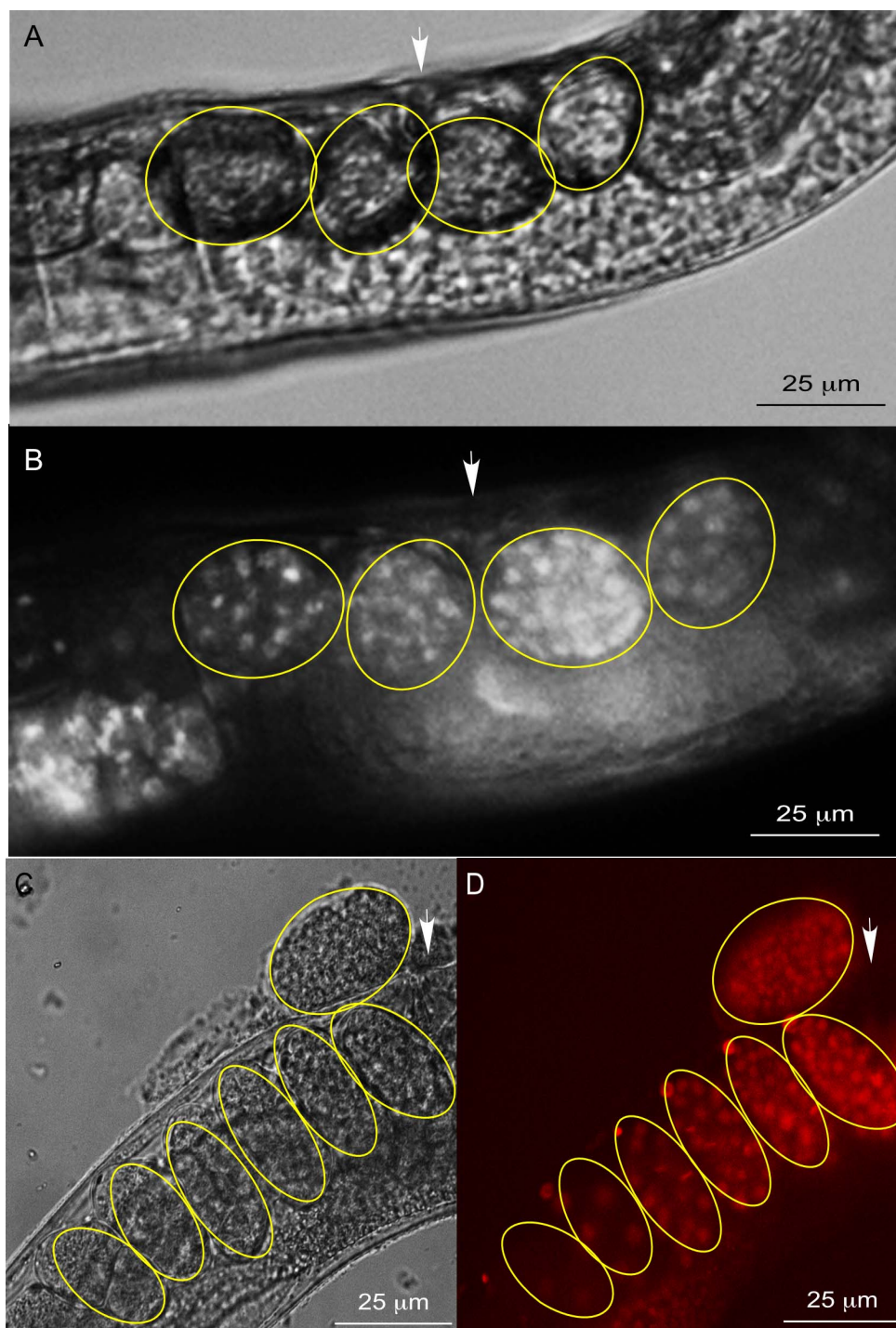
**Figure 10:** The results of the final phase of IUF trials. SL1699 males and SL1607 hermaphrodites were used in this trial. All photographs were taken using a dissecting microscope. The photographs are time-stamped in the top right corner of each figure (A-E), the yellow circles mark haploid pronuclei, and the cyan circles signify diploid nuclei. A-E provide a chronological development of the embryo during immediately after it was laid. These images were captured with an Olympus SXZ12 dissecting microscope.



**Figure 11:** Photos of the progeny formed from the embryos in Figure 10. Both embryos exhibited red pharynxes, confirming fertilization with a male-derived sperm. Since both worms exhibited a red pharynx, the paternity of the developing embryo is confirmed. These images were captured with an Olympus SXZ12 dissecting microscope.



**Figure 12:** Immature embryos laid from the final phase of IUF trials. All embryos exhibited red pharynxes as adults, confirming that they resulted from fertilization by a male-derived sperm. These images were captured with an Olympus SXZ12. dissecting microscope



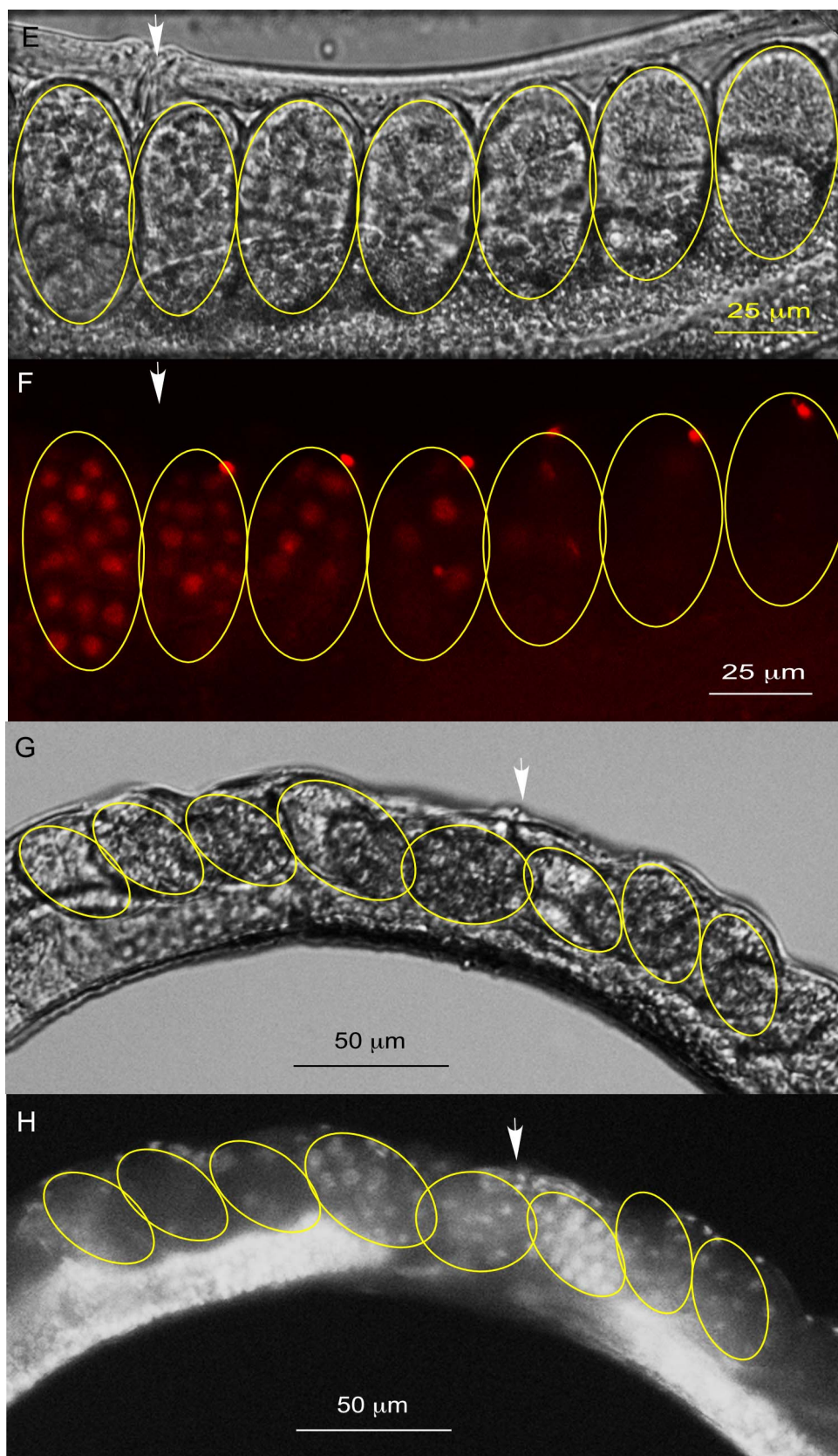


**Figure 13:** Fertile control worm strains with fluorescent markers. A and B show N2 wild-type worms. C and D show a fertile SL1655, E and F shows a fertile SL1699, and G and H show a fertile SL1607 hermaphrodites. Black and white images were taken using DIC, red images were taken with a TR filter, and B and H are DAPI. All worms exhibit well-developed embryos near the vulva.

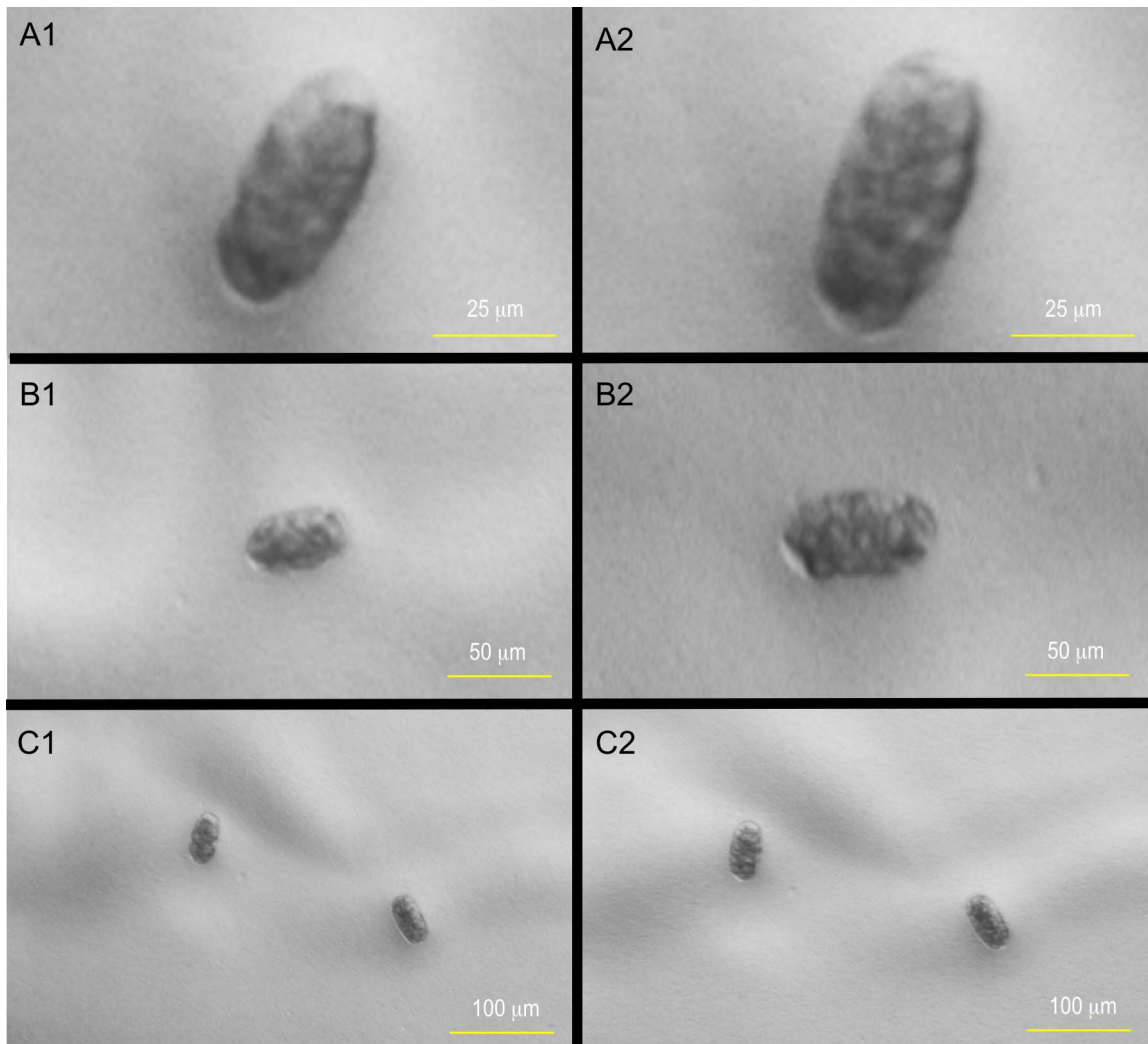


**Figure 14:** Embryos laid from fertile SL1607 hermaphrodites after being incubated at 25°C for one hour. These embryos resemble wild-type embryos near the vulva (Figure 13), and are a much later embryonic stage than those laid in the final phase of IUF trials. These images were captured with an Olympus SXZ12 dissecting microscope.

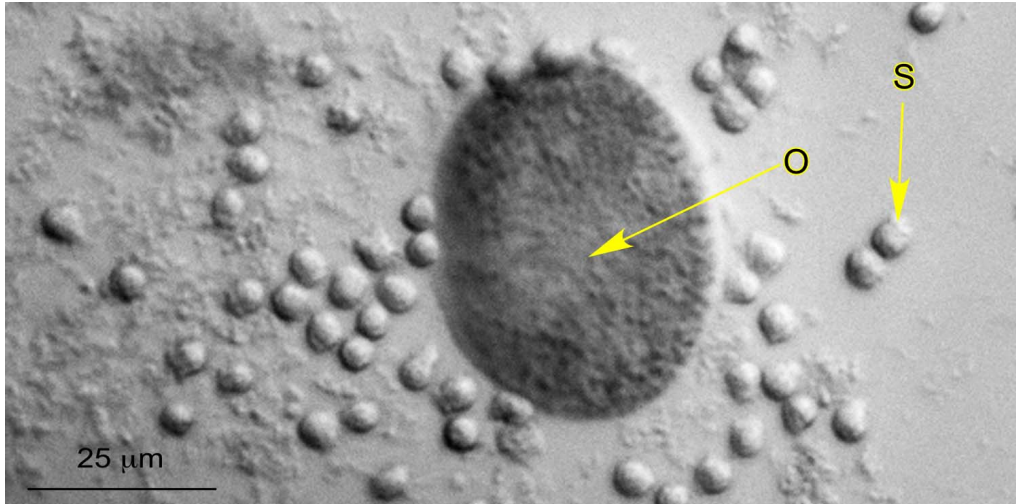


**Figure 15:** Activated sperm and a healthy oocyte in a final phase IVF trial. No embryonic activation or embryonic development was observed later. 'O' stands for oocyte and 'S' stands for sperm. This image was taken using DIC microscopy.

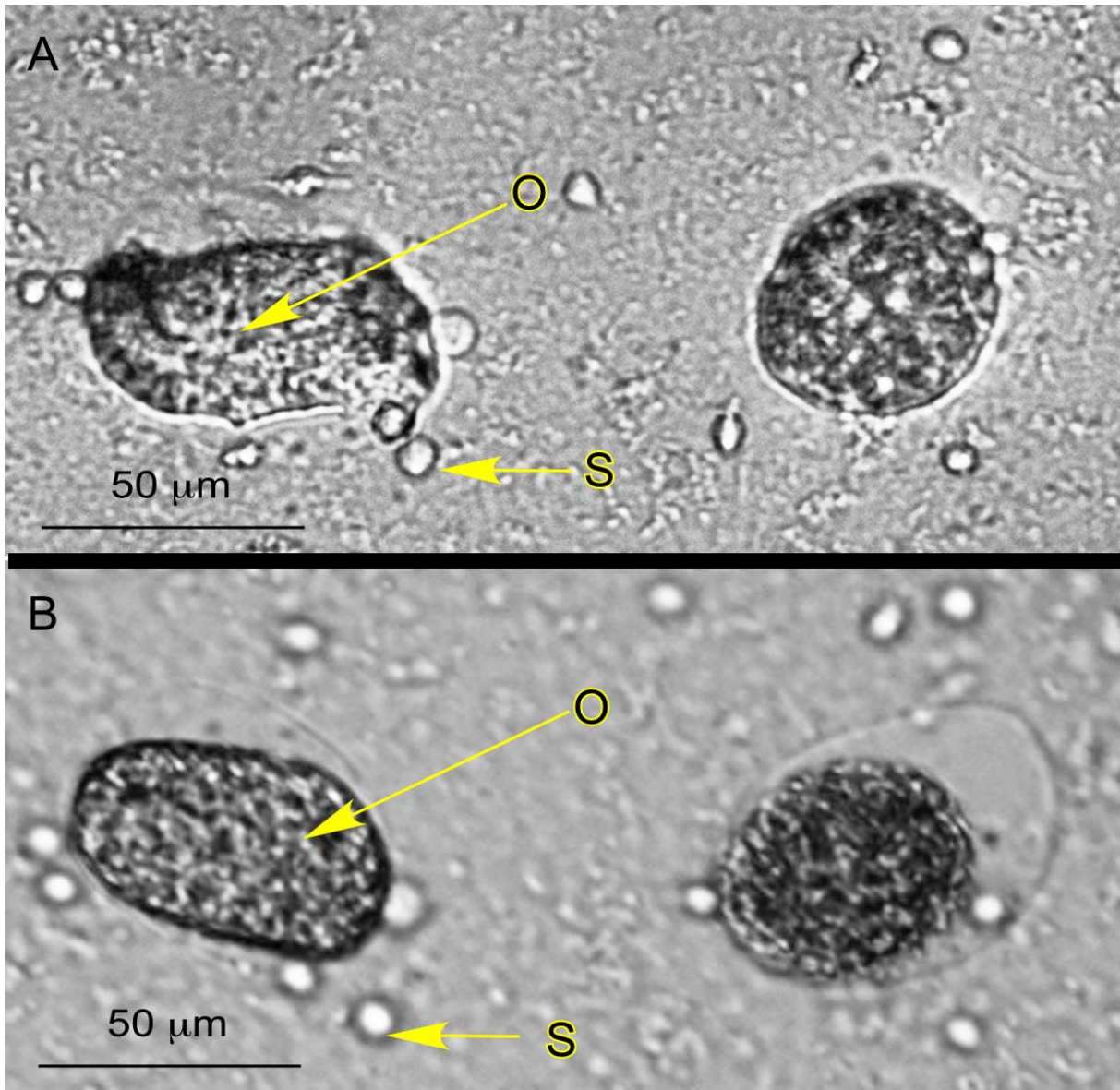


**Figure 16:** Oocytes from a last phase IVF trial. A and B are taken using DIC microscopy and are one day apart. As shown, the left oocyte shows distinct morphological changes that are similar to what an embryo undergoes, however no further development was observed. 'O' stands for oocyte and 'S' stands for sperm.

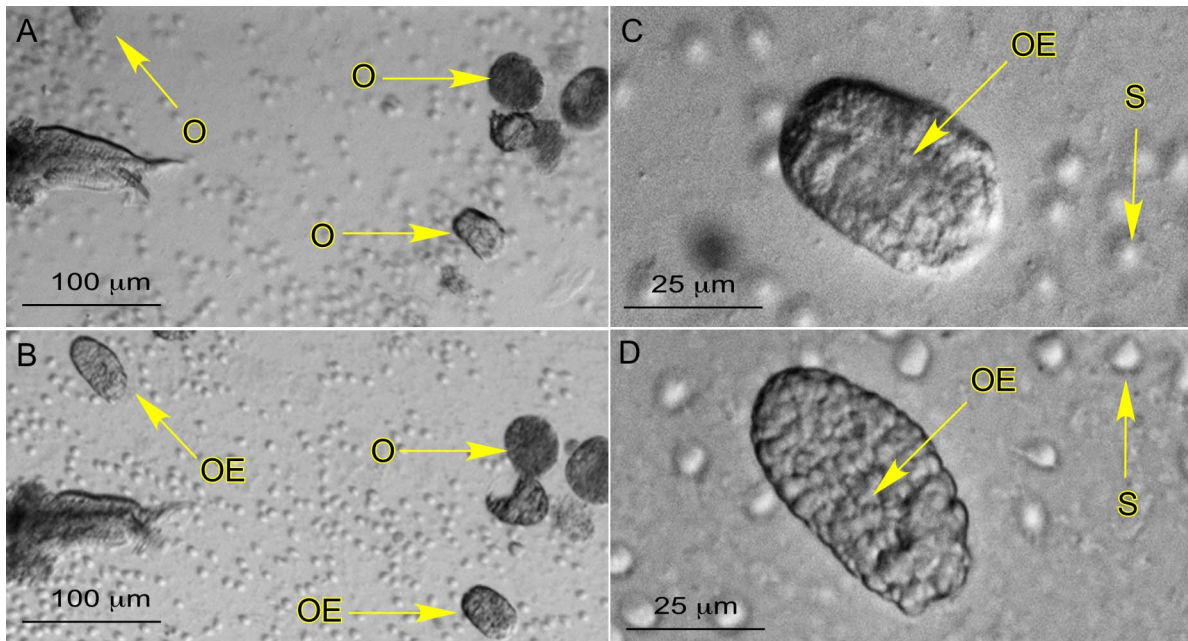


**Figure 17:** A shows initial pictures taken during a final phase IVF trial. B shows the conditions of the oocytes and embryos one day later. C and D exhibit two potential embryos observed on the second day, but no farther development occurred. 'O' stands for oocyte, OE stands for potential embryo, and 'S' stands for sperm. All pictures were taken using DIC microscopy.

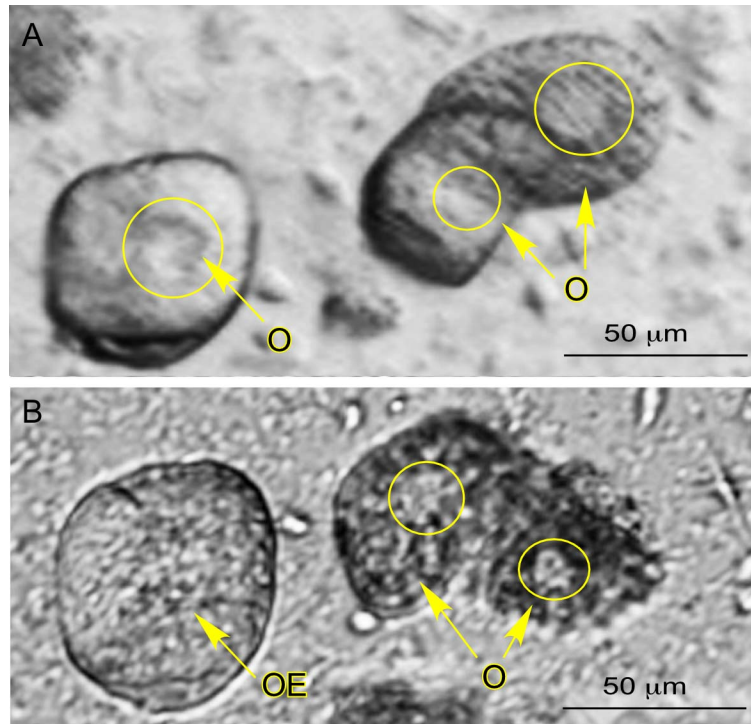


**Figure 18:** Shows the pronuclei of the left oocyte disappearing during a final phase IVF trial. The pronuclei are circled in yellow. Figure A and B were taken one day apart. 'O' stands for oocyte, OE stands for potential embryo, and 'S' stands for sperm. All pictures were taken using DIC microscopy.

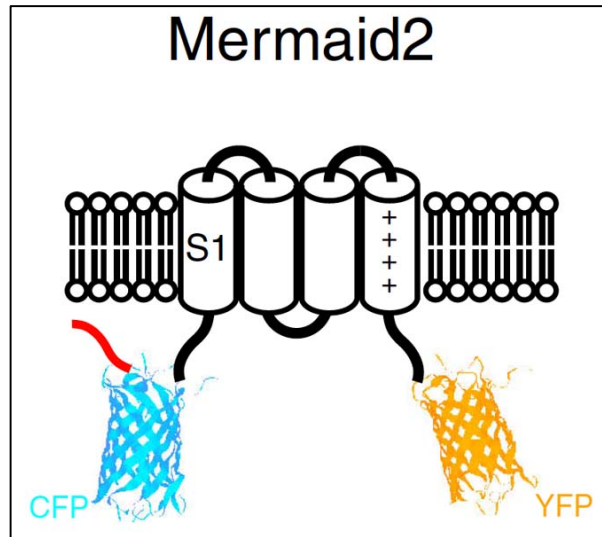


**Figure 19:** The Mermaid-2 voltage sensor. It is a transmembrane protein consisting of four domains (S1-S4). In addition, it also possesses CFP and YFP markers, as shown. This image is modified from Tsutsui et al., 2013.

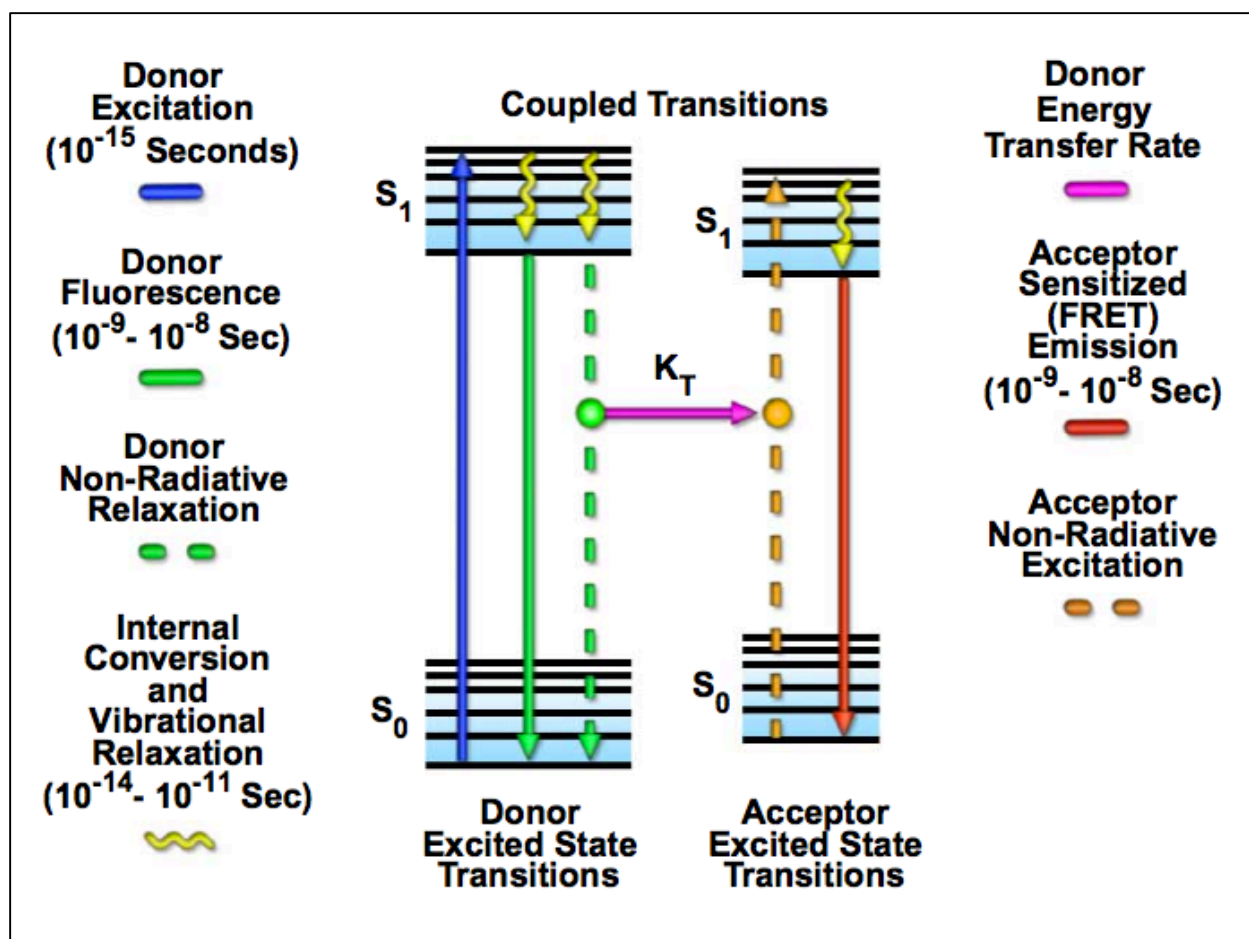


**Figure 20:** A diagram of the coupled dipoles between donor and receptor fluorophores in FRET.  $S_0$  indicates the ground energy level where  $S_1$  indicates a higher energy level. Absorption and emission lines are straight, continuous vertical lines. Vibrational relaxation is indicated by yellow squiggly lines. The coupled transitions are shown with dashed lines. In sum, the donor fluorophore transfers energy to the acceptor (pink line), resulting in excitation and a subsequent emission. This image is adapted from Kremers & Davidson, 2016.

| Primer | Function                        | Sequence   |
|--------|---------------------------------|--|
| EJG154 | Forward primer for <i>glh-2</i> | 5'- GGC CTG AGT ACA TGC GGC CTC GCG GTA CAA<br>GTT TGG CG -3'                            |
| EJG155 | Reverse primer for <i>glh-2</i> | 5'- TGA GTC GTA TTA CGT AGC CCG GAA TTC ATA TTA<br>CCA TTA TTC TTG AAC TTT TAT AGT C -3' |
| EJG156 | Forward primer for <i>fbf-2</i> | 5' - AGT CAA CGG CTG GGC CTC ATG ATA AGG TGG<br>AAC TTT CTC ACC ATA AAT C -3'            |
| EJG157 | Reverse primer for <i>fbf-2</i> | 5' - GAA TGT CTA GAA CTA GGC CCA AGA CTC GAA<br>CGA TAT TTT GCC AAG -3'                  |

**Table 21:** Sequence of primers used in PCR amplification during the synthesis of the Mermaid-2 vector pHP1. All primers were orders from Integrated DNA Technologies.

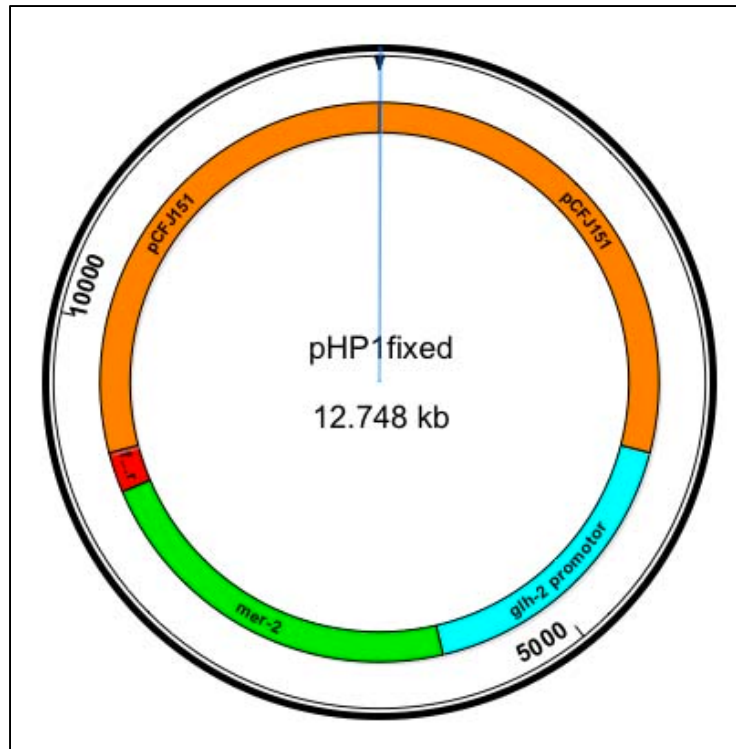


**Figure 22:** Shows the Mermaid-2 plasmid pHP1. The orange segment represents the vector backbone pCFJ151 (MosSCI); it is 7.4 kb. The purple section is the *glh-2* promoter; it is 2.2 kb. The green segment is Mermaid-2 excised from pEJG30; it is 2.8 kb. Lastly, the red section represents *fbf-2* 3'-UTR; it is 0.3 kb.

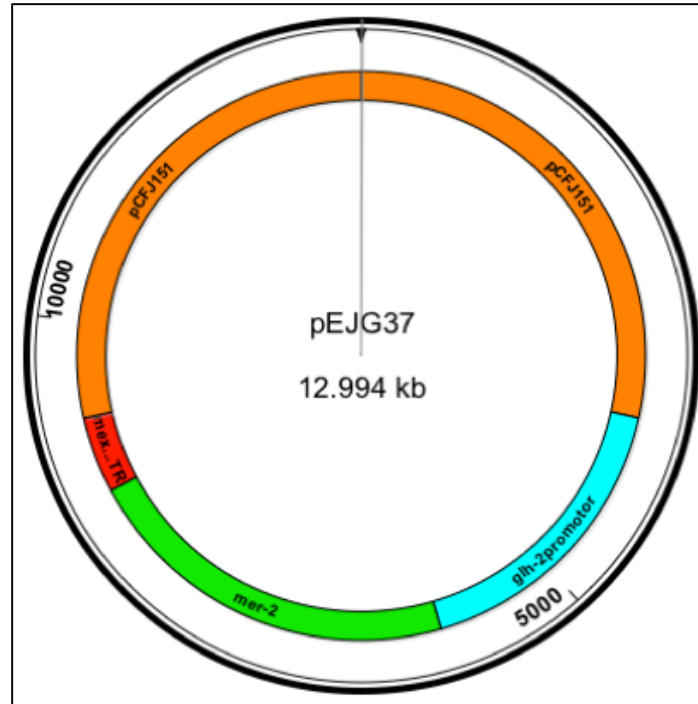


**Figure 23:** Shows the Mermaid-2 plasmid constructs pEJG37. Orange represents the pCFJ151 (MosSCI) vector backbone; it is 7.4 kb. The cyan segment represents the *glh-2* promoter; it is 2.2 kb. The green segment is the Mermaid-2 vector excised from pEJG30; it is 2.8 kb. Lastly, *mex-5* 3'-UTR is shown in red. It is 0.5 kb.

| <b>Primer</b> | <b>Function</b>                 | <b>Sequence</b>  |
|---------------|---------------------------------|--|
| EJG203        | Forward primer for <i>glh-2</i> | 5'- CCG TCG AAT CCC TCC ATA GGC GCG GTA CAA GTT<br>TGG CG - 3'                           |
| EJG206        | Reverse primer for <i>glh-2</i> | 5'- TGA GTC GTA TTA CGT AGC CCG GAA TTC ATA TTA<br>CCA TTA TTC TTG AAC TTT TAT AGT C -3' |
| EJG204        | Forward primer for <i>mex-5</i> | 5' - AGT CAA CGG CTG GGC CTC ATT AGG TTG TAT<br>GTT AAC ACA C -3'                        |
| EJG205        | Reverse primer for <i>mex-5</i> | 5' – GAA TGT CTA GAA CTA GGC CCA TAA TCT TTG<br>CAC CAT TTA TTG -3'                      |

**Figure 24:** Sequences of primers used in the synthesis of the Mermaid-2 vector pEJG37. All primers were ordered from Integrated DNA Technologies.

gtaccctctagtcaaggccttaagtgagtcgtattacgtagcccggaattcatattaccattattcttgaacttttatagtctttgtagtggt  
 ttcgtgtagaaggcattggagtcgaaaggttgaaagtggttcagaagaatccgagtcgaaatgaatcccagaatctacaaaaactttt  
 attaaacaatttagagcttttgagagtgcatgttaaattgcattcataactgtttgttatctgtttctactaattagttccaccgaatcagg  
 atgcagtgagcgaaccgaaatcgtgaattcggtttcgccacaggggacgaaaagtaggttactaatatgtgaagcttttaaaaactc  
 cataaatttgtgaactccacagctaggatcaagggtgccgattatcgttttcaggaaaacattttttgtttacattttccgcggttaa  
 aagttgagggtttctcgttttagaataaattcatgtttccttaatttttttcatcaacacaaaaaattgattattaacattttcttaaaa  
 atttccgatttttcgttttcaggaaaatcgaaatttttcgctttccgatatttcgaaaaatatttcatttttagagttatcttctttttaga  
 agaaaattatgtttctatgattttcccatcaacaaaaaataatttttgaaactgattttctttgtaactttctaaattttttattttc  
 aggaaaatcgaaacatcgaaattgttcattttcatgataccctaaaaataaagtttgatcgatataatctatttcaatcttatgaaa  
 ttttaaaataaactgaccagaatcggatgtgcttcggtagctgagaggtccattgttcttctcatcgacttcatcatcactatcttctc  
 aatcgttgttactaccattgtttccaaccaattttcattgcacttgaaatttcaagggttcatactactttgatacattccaatgccg  
 aattatgctcgttagtcatcaaatcctcagcaggagaacacccatccgagaaggaatactttcaaaaaccaacagagaataaactttgat  
 tttccatatacaatccagaagactttagtattggtctgaaatctggctgcagcgagtttcagagttacagcgagcaaaatcatat  
 tgtatcagagccgtgaagtagtgaatttcttgatgaaaccagttttgaaagctgttgagaatgaaaatgttcatcgcaaggttttca  
 gcatacttgaagcgtcacgtgggttcagaatgagtttccgtccgtaagatctcaatcaacgtttcagtgtaagctctggtgtgtgac  
 atactgcaatttttaattgaaggcaaaatttgatgttcaacaaaattacgttgaaaatcgccgtccgaatcgcgatacttcgttaaaat  
 gaacgttgaatgaccgaagggtgaagaatacaagctaaacgtcgttggcagttattcgtgatgaacccttaagaatattgtttaa  
 tttggccaaattcagagttattaccattgaatcagaagttgaataatccatgattttctccataggcaacgggttcgacattgcaatc  
 attgattggcatgaaatgtgtccatatacgtcgtccttcattgtatggcttctcagtgactcgataattttttcgcgaggggttcgattccat  
 ccttgctttgataatactgagttatgtggctgagaagaactcctcctcctcggacgaggcaaatagtcttgattgaaagttcgttgaga  
 gcatgaattgcgtccagtacactaatattcatttctgaaaaaataataaattgaaatgaaatgcaaaaagataaacgaacgtttaa  
 gtttaaaaaggtctccagattaattagggaaactattttcagaagaaaaaattcgaaggttcacaaagtattactggtatggcaaaaa  
 gtgcgatgcaaggatactgaaattgtattcagaaaatccaaattgagtttttaaaaggctcatacagcagcataggacaagggtctcg  
 ccagttcgtcctctacagtactcccgcgaggcaaaattcaaatcttttcgcgcgagtttctgagtttcattcattaaaaatttttggttg  
 caaacgcaaaactgtaccgacct**M E G F D G S D F S P P A D L V G**  
**ATGGAGGGATTTCGACGGTTCGACTTCTCCACCAGCTGACCTTGTTGG**  
**V D G A V M R N V V D V T I N G D V T A P P K**  
**AGTTGACGGTGCAGTCATGCGTAACGTCGTTGACGTCACGATCAACGGTGACGTCCTGCTCCGCCGAA**  
**A V A P R K S E S V K K V H W N D V D Q G P S**  
**GGCTGCGCCACGCAAATCCGAGTCGGTAAAGAAAAGTTCACTGGAACGATGTAGACCAGGGACCGTCCG**  
**E K P E T R Q E E R I D I P E I S G L W W G E**  
**AAAAGCCAGAGACGAGACAGGAGGAACGCATCGACATACCAGAGATCTCCGGTCTATGGTGGGGAGA**  
**N E H G V D D G R M E I P T T G V G**  
**GAACGAG CACGGAGTCGACGATGGAAGAATGGAGATACCAACTACTGGTGTAGG**taagtttatcgtttttcga  
 cgattttaccatttttacgccatttttgataactaactaacgcctttttaccgatttttcag**D P M V S K G**  
**GGACCCAATGGTGTCCAAGGGAG**  
**E E L F T G V V P I L V E L D G D V N G H R F**  
**AGGAGCTTTTCACCGGAGTCGTCCCAATCCTTGTGAGCTTGACGGCGACGTAACCGACACCGCTTCA**  
**S V R G E G E G D A T Q G K L T L K F I C T T**  
**GCGTGCCTGGAGAGGGAGAGGGAGACGCCACCCAGGGCAAGCTTACCCTTAAGTTTCATCTGCACCACC**  
**G K L P V P W****P T L**  
**GGCAAGTTGCCAGTGCCATGG**gtaagtttaacatataataactaactaacctgattatttaattttcag**CCAACCCTCG**  
**V T T L S W G V Q C F A R Y P D H M K Q H D F F**



R T I F F K D D G N Y K T  
 GAACTATTTCTTTAAGGATGATGGAACTACAAGACAAgtaagttaaactacatgctactaactaacgtcattaattt  
 R A E V K F E G D T L V N R I E L K G I D  
 aaatttcagGGGCTGAAGTCAAATTTGAAGGAGATACACTCGTCAACCGCATCGAACTCAAAGGAATTGA  
 F K E D G N I L G H K L E Y N Y N S H N V Y I  
 CTTTAAAGAGGATGGAAATATTCTCGGCCATAAACTCGAATATAATTACAATTCCCATAATGTCTACATTA  
 T A D K Q K N G I K A  
 CCGCTGATAAACAGAAAAACGGAATTAAGCTAgtaagttaaactcgagaataactaactaacatataagcatttaaattt  
 N F K I R H N I E D G G V Q L A D H Y Q Q N T  
 cagATTTCAAATCAGACATAATATCGAAGATGGAGGAGTCCAACCTTGCTGATCATTATCAACAGAATAC  
 P I G D G P V L L P D N H Y L S Y Q S A L S K  
 CCAATTGGAGATGGACCAGTCTCCTCCTGATAATCATTATCTCTCCTATCAAAGCGCACTCTCCAAGG  
 D P N E K R D H M V L L E F V T A A G I T L G  
 ACCCGAATGAGAAGAGGGACCACATGGTCTCCTCGAATTTGTCACCGCTGCTGGAATTACCTTGAA  
 M D E L Y K  
 TGGACGAACTCTATAAAtaaactagtcaacggctgggctcattaggtgtatgttaccacacgaaattgcttttcatgtactattg  
 tctgtacataccgcctctcttttctctacacaacttttttcaaaattcattcaagcttgaccaccaatcacacaaactcattca  
 aatcatctaaatttcatacttactaatttcgaagtaacaggtctcagctttcaacaacattttaccagcttctgtgccttttaccg  
 attttccacatagcaaaattatctttatccggattttattccaatatgttttttcaaatcccacccaattgtttaccatttcaccatt  
 cctggcccaaatcactttgtgagtcaccaacataatctaataagaatgttgacatccagcctctccacctcttacctcaaaact  
 atctagcatgtcggccttgatcggctgacaatatatagttttttctttcccttctcaatttttccatctccccaccgccaagagt  
 tcttccatagagattgttcaactccaataaatgggtgcaagattatgggctagtctagacattcttaataaaaaatctttcagttga  
 aattgaaaatgagttaaagtggagtttttattgaaaacagatttccgtgtgattagtttttagcgagtgtagaggacagcgaaaaa  
 tatagaacaaggggggaactgaaaagcttaggaatgcattgaacatgagaaggggaaggggaaggaacaaactagacaggaatta  
 ttggaatttaacacatttgagttttttctattcgacagaataattatccagaacattttgtattaaatattatgcatcatatgagtagt  
 cggctttgtgtcatgacgagttttatcgacgaaatagaagctgtcagaacgagctcgtttggattgttgatcatgtcgtccactgaa  
 aaagagattagcttttgaattgtactttttagaataatgactcactgagttgttgagagagttgaggaactcatagatatgttcacagtt  
 gtttctgtaattcggaaacagaatccgaattcaaagtcaaaacacttcagaaggcgatctttgaagaagtgcggttcgatcattcggaa  
 atgatggattgggatgtctcactttgaattccacagttgctccgacctttgagtttcaaaaagttggagcaaatctataacgcacgt  
 atcttccgactcctgtggcgactcatcattctctgatcttccggtttggcgatctcgaagcacttgctcagtgccagatcacgga  
 tttggaacttggtgaactcgatgttatagatgttcgcagatggggagcataagaatcctaaattatgt

**Figure 25:** The DNA sequence of *glh-2*, Mermaid-2, and *mex-5* present in pEJG37.

Blue font indicates the *glh-2* promoter. Red font indicates the *mex-5* (3'-UTR). CFP and YFP amino acids are highlighted by their respective colors. Mermaid-2 exons are highlighted in a red, and their corresponding amino acids are centered above each codon. Note that if a codon appears incomplete, it is due to splicing and one only needs to examine the downstream sequence to find the rest of the codon.

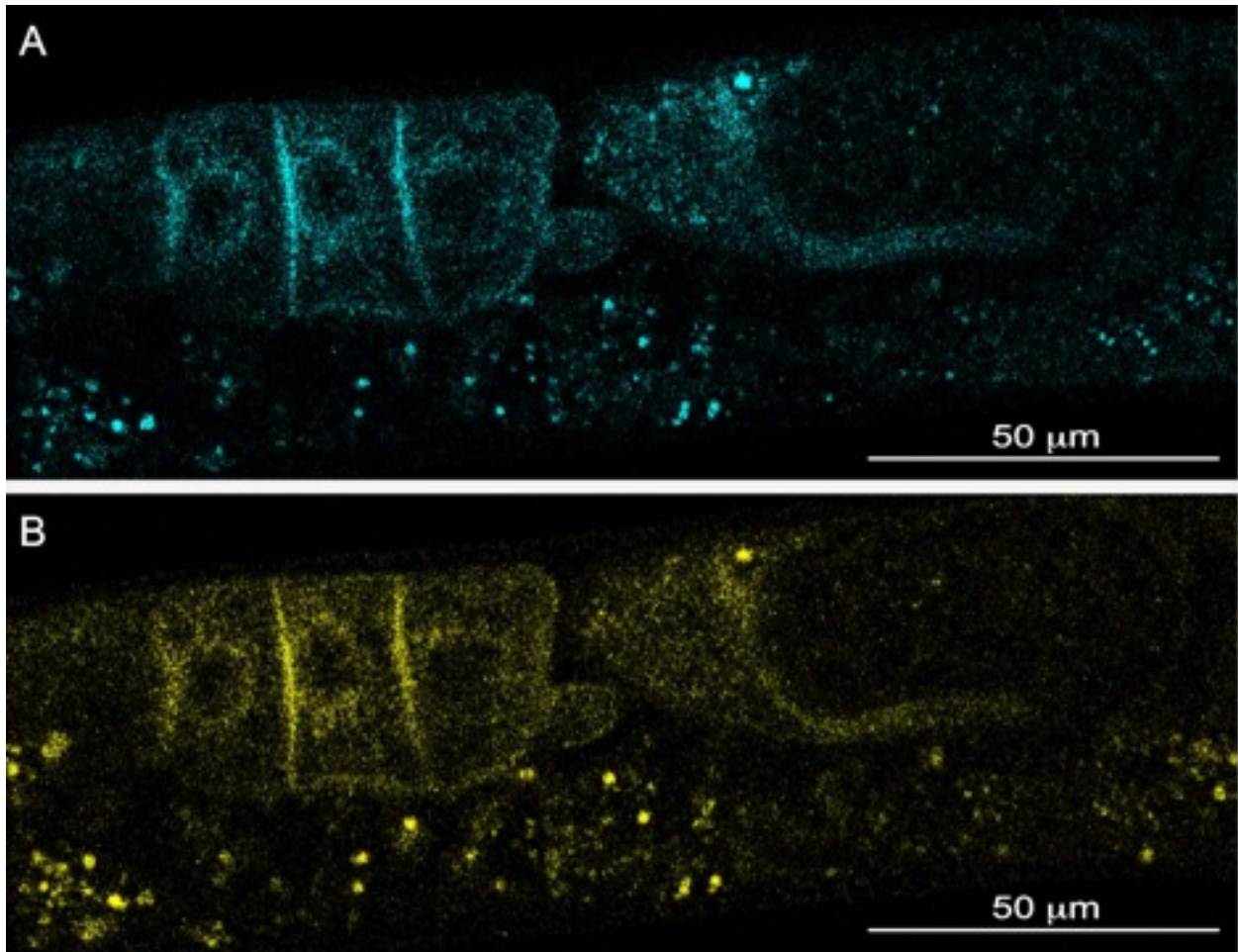


**Figure 26:** Shows the activity of the Mermaid-2 voltage probe. A, CFP expression; B, YFP expression. The detection of yellow fluorescence confirms FRET between the two fluorophores. These images were taken with a Leica TCS SP8 Confocal Microscope

## References

1. Corsi, A.K., B. Wightman, and M. Chalfie, *A Transparent Window into Biology: A Primer on C. elegans*. WormBook, 2015: p. 1-31.
2. Porta-de-la-Riva, M., et al., *Basic C. elegans methods: synchronization and observation*. J Vis Exp, 2012(64): p. e4019.
3. Hu, P.J., *Dauer*. WormBook, 2007: p. 1-19.
4. Griffiths, A., J. Miller, and D. Suzuki, *An Introduction to Genetic Analysis*. 7th ed. 2000, New York, NY: W. H. Freeman and Company.
5. Hodgkin, J., H.R. Horvitz, and S. Brenner, *Nondisjunction Mutants of the Nematode C. elegans*. Genetics, 1979. **91**(1): p. 67-94.
6. Nishimura, H. and S.W. L'Hernault, *Spermatogenesis-defective (spe) mutants of the nematode C. elegans provide clues to solve the puzzle of male germline functions during reproduction*. Dev Dyn, 2010. **239**(5): p. 1502-14.
7. L'Hernault, S.W., *Spermatogenesis*. WormBook, 2006: p. 1-14.
8. Ward, S., Y. Argon, and G.A. Nelson, *Sperm morphogenesis in wild-type and fertilization-defective mutants of C. elegans*. J Cell Biol, 1981. **91**(1): p. 26-44.
9. Liu, Z., et al., *The micronutrient element zinc modulates sperm activation through the SPE-8 pathway in Caenorhabditis elegans*. Development, 2013. **140**(10): p. 2103-7.
10. McCarter, J., et al., *On the control of oocyte meiotic maturation and ovulation in C. elegans*. Dev. Biol, 1999. **205**: p. 111-128.
11. Singson, A., K.L. Hill, and S.W. L'Hernault, *Sperm competition in the absence of fertilization in C. elegans*. Genetics, 1999. **152**(1): p. 201-8.
12. Ting, J.J., et al., *Intense sperm-mediated sexual conflict promotes reproductive isolation in C. elegans*. PLoS Biol, 2014. **12**(7): p. e1001915.
13. Pohl, K., *The Identification and Mapping of a Gene Responsible for a Novel nonEmo Phenotype in C. elegans Oocytes*, Honors Thesis, Emory University. 92 pp.
14. Ikawa, M., et al., *Fertilization: a sperm's journey to and interaction with the oocyte*. J Clin Invest, 2010. **120**(4): p. 984-94.
15. Okabe, M., *The cell biology of mammalian fertilization*. Development, 2013. **140**(22): p. 4471-9.
16. Gilbert, S.F., *Developmental Biology* 6th ed. 2000, Sunderland, MA: Sinauer Associates.
17. Campbell, N.A. and J.B. Reece, *Biology*. Seventh ed. 2005: Pearson.
18. Singson, A. and M.R. Marcello, *Fertilization and the oocyte-to-embryo transition in C. elegans*. BMB reports, 2010. **43**(6): p. 389-399.
19. Hodgkin, J. and T. Doniach, *Natural variation and copulatory plug formation in Caenorhabditis elegans*. Genetics, 1997. **146**(1): p. 149-64.
20. Brenner, S., *The Genetics of C. elegans*. Genetics, 1974. **77**(1): p. 71-94.
21. Ward, S. and J.S. Carrel, *Fertilization and sperm competition in the nematode C. elegans*. Dev Biol, 1979. **73**(2): p. 304-21.
22. Goldstein, B. *Embryogenesis of C. elegans*. [Video] 2003; Available from: <http://wormclassroom.org/embryogenesis-c-elegans>.
23. Lints, R. and D.H. Hall. *Reproductive system, egg-laying apparatus*. 2009 February 1, 2013 [cited 2017 March 6]; Available from: <http://www.wormatlas.org/hermaphrodite/egg-laying-apparatus/mainframe.htm>.
24. Johnson, M., *Robert Edwards: the path to IVF()*. Reproductive Biomedicine Online, 2011. **23**(2): p. 245-262.
25. Chang, M.C., *Fertilization of Rabbit Ova in vitro*. Nature, 1959. **184**(4684): p. 466-467.

26. Brackett, B., *Assisted Fertilization and Nuclear Transfer in Mammals*. 1 ed. 2001, Totowa, NJ: Humana Press.
27. Kamel, K.R., *Assisted Reproductive Technology after the Birth of Louise Brown*. *Journal of Reproduction & Infertility*, 2013. **14**(3): p. 096-110.
28. McCarter, J., et al., *Soma-germ cell interactions in C. elegans: multiple events of hermaphrodite germline development require the somatic sheath and spermatheca lineages*. *Dev Biol*, 1997. **181**(2): p. 121-43.
29. Lee, E., *Investigating the expression of PEZO-1 protein and its involvement with the Emo oocyte phenotype in C. elegans*, Honors Thesis. 2016, Emory University. 63 pp.
30. Nelson, G.A. and S. Ward, *Vesicle fusion, pseudopod extension and amoeboid motility are induced in nematode spermatids by the ionophore monensin*. *Cell*, 1980. **19**(2): p. 457-64.
31. Ward, S., E. Hogan, and G.A. Nelson, *The initiation of spermiogenesis in the nematode C. elegans*. *Dev Biol*, 1983. **98**(1): p. 70-9.
32. LaMunyon, C.W. and S. Ward, *Assessing the viability of mutant and manipulated sperm by artificial insemination of C. elegans*. *Genetics*, 1994. **138**(3): p. 689-92.
33. Bae, Y., et al., *The CIL-1 PI 5-phosphatase localizes TRP Polycistins to cilia and activates sperm in C. elegans*. *Curr Biol*, 2009. **19**: p. 1599-1607.
34. Shaham, S., *Methods in cell biology*. WormBook: The Online Review of *C. elegans* Biology, 2006.
35. Machaca, K., L. DeFelice, and S.W. L'Hernault, *A novel chloride channel localizes to C. elegans spermatids and chloride channel blockers induce spermatid differentiation*. *Developmental biology*, 1996. **176**(1): p. 1-16.
36. Zhang, S. and J. Kuhn, *Cell isolation and culture*. WormBook: The Online Review of *C. elegans* Biology, 2013: p. 1-39.
37. Smith, J. and G. Stanfield, *TRY-5 Is a sperm-activated protease in C. elegans Seminal Fluid*. *PLoS Genetics*, 2011. **7**(11).
38. Shelton, C.A. and B. Bowerman, *Time-dependent responses to glp-1-mediated inductions in early C. elegans embryos*. *Development*, 1996. **122**(7): p. 2043-50.
39. Singaravelu, G., et al., *Isolation and in vitro activation of C. elegans sperm*. *J Vis Exp*, 2011(47).
40. Burruano, B.T., R.L. Schnaare, and D. Malamud, *Synthetic cervical mucus formulation*. *Contraception*, 2002. **66**: p. 137-140.
41. Han, S.M., P.A. Cottee, and M.A. Miller, *Sperm and oocyte communication mechanisms controlling C. elegans fertility*. *Dev Dyn*, 2010. **239**(5): p. 1265-81.
42. Ward, G., et al., *Chemotaxis of Arbacia punctulata spermatazoa to resact, a peptide from the egg jelly layer*. *The Journal of Cell Biology*, 1985. **101**: p. 2324-2329.
43. Gardner, A.J., C.J. Williams, and J.P. Evans, *Establishment of the mammalian membrane block to polyspermy: evidence for calcium-dependent and -independent regulation*. *Reproduction*, 2007. **133**(2): p. 383-93.
44. Jaffe, L., *Electrical polyspermy block in sea urchins: nicotine and low sodium experiments*. *Development, Growth, and Differentiation*, 1980. **22**(3): p. 503-507.
45. Eisen, A., et al., *Temporal sequence and spatial distribution of early events of fertilization in single sea urchin eggs*. *Journal of Cell Biology*, 1984. **99**: p. 1647-1654.
46. Eddy, E. and B. Shapiro, *Membrane events of fertilization in sea urchin*. *Scan Electron Microscopy*, 1979. **3**: p. 287-97.
47. Inoue, N., M. Ikawa, and M. Okabe, *Putative sperm fusion protein IZUMO and the role of N-glycosylation*. *Biochem Biophys Res Commun*, 2008. **377**(3): p. 910-4.
48. Jaffe, L., A. Sharp, and D. Wolf, *Absence of an electrical polyspermy block in the mouse*. *Developmental Biology*, 1983. **96**: p. 317-323.

49. Parry, J.M., et al., *EGG-4 and EGG-5 Link Events of the Oocyte-to-Embryo Transition with Meiotic Progression in C. elegans*. *Curr Biol*, 2009. **19**(20): p. 1752-7.
50. Tsutsui, H., et al., *Improving membrane voltage measurements using FRET with new fluorescent proteins*. *Nat Methods*, 2008. **5**(8): p. 683-5.
51. Hille, B., *Ion Channels of Excitable Membranes*. 3 ed. 2001, Sunderland, MA 01375: Sinauer Associates, Inc.
52. Tsutsui, H., et al., *Improved detection of electrical activity with a voltage probe based on a voltage-sensing phosphatase*. *J Physiol*, 2013. **591**(18): p. 4427-37.
53. Kremers, G.J. and M.W. Davidson. *Basics of FRET Microscopy*. 2016 [cited 2017].
54. Lakowicz, J.R., *Principles of Fluorescence Spectroscopy*. 2 ed. 1999, New York, NY: Plenum Publishing Corp.
55. Clegg, R.M., *Fluorescence resonance energy transfer*. Vol. 137. 1996, New York, NY: John Wiley & Sons Inc.
56. Förster, T., *Delocalized excitation and excitation transfer*. Vol. 3. 1965, New York, NY: Academic Press, Inc.
57. Sekar, R.B. and A. Periasamy, *Fluorescence resonance energy transfer (FRET) microscopy imaging of live cell protein localizations*. *J Cell Biol*, 2003. **160**(5): p. 629-33.
58. Tsutsui, H., et al., *Visualizing voltage dynamics in zebrafish heart*. *The Journal of Physiology*, 2010. **588**(Pt 12): p. 2017-2021.
59. Bowman, E.A., et al., *Phosphorylation of RNA polymerase II is independent of P-TEFb in the C. elegans germline*. *Development*, 2013. **140**(17): p. 3703-13.
60. Gibson, D.G., et al., *Enzymatic assembly of DNA molecules up to several hundred kilobases*. *Nat Methods*, 2009. **6**(5): p. 343-5.
61. Lynn, J.W. and E.L. Chambers, *Voltage clamp studies of fertilization in sea urchin eggs. I. Effect of clamped membrane potential on sperm entry, activation, and development*. *Dev Biol*, 1984. **102**(1): p. 98-109.
62. Frokjaer-Jensen, C., et al., *Single-copy insertion of transgenes in C. elegans*. *Nat Genet*, 2008. **40**(11): p. 1375-83.
63. Tenlen, J.R., et al., *MEX-5 asymmetry in one-cell C. elegans embryos requires PAR-4- and PAR-1-dependent phosphorylation*. *Development*, 2008. **135**(22): p. 3665-75.
64. Mello, C. and A. Fire, *DNA transformation*. *Methods Cell Biology*, 1995. **48**: p. 451-482.
65. Robert, V.J., N.L. Vastenhouw, and R.H. Plasterk, *RNA Interference, Transposon Silencing, and Cosuppression in the C. elegans Germ Line: Similarities and Differences*. *Cold Spring Harbor Symposia on Quantitative Biology*, 2004. **69**: p. 397-402.